Regulation of the Human Prostacyclin Receptor Gene in Megakaryocytes: Major Roles for C/EBPδ and PU.1.

Garret L. Keating, Elizebeth C. Turner and B. Therese Kinsella*

UCD School of Biomolecular and Biomedical Sciences, UCD Conway Institute of Biomolecular and Biomedical Research, University College Dublin, Belfield, Dublin 4, Ireland.
*Corresponding author: Tel: 353-1-7166727; Fax 353-1-7166456
Email: Therese.Kinsella@UCD.IE

Running Title: Regulation of the Prostacyclin Receptor Gene

Abbreviations: CAD, coronary artery disease; C/EBP, CCAAT/enhancer binding protein; ChIP, chromatin immunoprecipitation; COX: cyclooxygenase; C-LH, cut-like homeodomain; CVD, cardiovascular disease; DMSO, dimethyl sulfoxide; ERE, estrogen response element; FBS, fetal bovine serum; HEL, human erythroleukemia; hIP, human prostacyclin receptor; IgG, immunoglobulin G; IP, prostacyclin receptor; Nrf, Nuclear respiratory factor; PMA, phorbol 12-myristate 13-acetate; pGL3B, pGL3Basic; pRL-TK, pRL-thymidine kinase; PRR, PMA-responsive region; QT, quantitative reverse-transcriptase; RLU, relative luciferase unit; SEM, standard error of the mean; SNP, single-nucleotide polymorphism; STAT, Signal Transduction And Transcription; TI, transcription initiation; SDM, site-directed mutagenesis; TX, thromboxane; URR, upstream repressor region.

Abstract:
The prostanoid prostacyclin plays a central role in haemostasis and vascular repair. Recent studies investigating the regulation of the human prostacyclin receptor (hIP) gene identified an upstream repressor region (URR) within its regulatory promoter, herein termed the PrmIP. This study aimed to identify the main *trans*-acting factors that bind within the URR to transcriptionally repress PrmIP-directed gene expression in the megakaryoblastic human erythroleukemia (HEL) 92.1.7 cell line. Of the putative *cis*-acting elements examined, disruption of C/EBP and PU.1 elements within the URR substantially increased PrmIP-directed gene expression. Chromatin immunoprecipitation (ChIP) confirmed that C/EBPδ and PU.1, but not C/EBPβ, bind to the URR *in vivo*, while ectopic expression of C/EBPδ substantially reduced hIP mRNA levels and PrmIP-directed gene expression. Phorbol 12-myristate 13-acetate (PMA)-induced megakaryocytic differentiation increased hIP mRNA and PrmIP-directed reporter gene expression and hIP-mediated cAMP generation in HEL cells. Two PMA-responsive regions, termed PRR1 and PRR2, were identified within PrmIP. Disruption of C/EBPδ and PU.1 *cis*-elements within the overlapping PRR1/URR and of Sp1, PU.1 and Oct-1 *cis*-elements within the overlapping PRR2/core PrmIP, revealed that both PRR1 and PRR2 contribute to the PMA- induction of hIP mRNA and gene expression in HEL cells. Furthermore, ChIP analysis established that induction of PrmIP-directed gene expression during megakaryocytic differentiation is largely regulated by PMA-induced dissociation of C/EBPδ and enhanced binding of PU.1 to PRR1 in addition to increased binding of Sp1, PU.1 and Oct-1 to elements within the core promoter/PRR2 *in vivo*. Taken together, these data provide critical insights into the transcriptional regulation of the hIP gene within the vasculature, including during megakaryocytic differentiation.

Key Words: prostacyclin receptor, C/EBP, Sp1, PU.1, Oct-1, promoter

1. INTRODUCTION:

Prostacyclin, also referred to as prostaglandin (PG) I_2, is a member of the prostanoid family of bioactive lipids derived from arachidonic acid through the sequential actions of cyclooxygenase (COX)-1/2 and prostacyclin synthase [1, 2]. Prostacyclin primarily signals through its cognate receptor referred to as the IP, a G-protein coupled receptor (GPCR), to mediate a diversity of physiologic actions. Within the vasculature, it serves as a potent vasodilator and is the major inhibitory prostanoid in platelet aggregation where its actions generally oppose those of thromboxane (TX) A_2 [3-5]. Hence, alterations or imbalances in the levels of prostacyclin and/or TXA_2 or of their specific synthases or receptors (IP and TP, respectively) have been implicated in a wide range of vascular disorders including thrombosis, stroke, myocardial infarction, atheroschlerosis and systemic or pulmonary hypertension [6-8]. Consistent with this, $IP^{-/-}$ null mice display enhanced thrombotic tendency in response to endothelial damage [9, 10]. Furthermore, $IP^{-/-}$ mice exhibit diminished pain perception and substantially reduced acute inflammatory responses, highlighting additional roles for prostacyclin in nociception and as a potent pro-inflammatory mediator [9-11]. Prostacyclin also acts as a critical protective agent against coronary artery disease (CAD) [12], mediated at least in part through its inhibition of leukocyte-endothelial cell interaction [13] and its promotion of endothelial cell survival and proliferation, supporting neovascularisation and angiogenesis [4, 5, 14]. Additionally, a recent study established that transcriptional expression of the human (h) IP is directly up-regulated by estrogen, suggesting that some of the known cardioprotective effects of estrogen within the female vasculature may be mediated through its ability to regulate hIP expression levels within the vasculature [15].

In keeping with the diverse actions of prostacyclin, the hIP is widely expressed throughout the vasculature, including in platelets/megakaryocytes, macrophages, vascular endothelial and smooth muscle cells, as well as in the heart, lung, kidney and sensory neurons of the dorsal root ganglion [1, 9, 10]. The hIP is primarily coupled to Gs- activation of adenylyl cyclase, mediating prostacyclin inhibition of platelet aggregation and vascular tone, but may also regulate a number of other secondary effectors [16, 17]. The hIP itself is subject to complex regulation through post-translational lipid modifications including isoprenylation and palmitoylation that greatly influence its primary signalling and functional expression [18-20]. Processing of the newly synthesized hIP is proofed by the unfolded protein response (UPR), while the functionally mature hIP undergoes agonist-induced trafficking through a Rab5a- and Rab11a-dependent mechanism involving a direct interaction between the hIP with Rab11a [21-25]. More recently, it has been established that the hIP can also directly interact with multi- Postsynaptic density-95, Discs large, Zonula occludens-1 (PDZ) domain containing protein PDZ domain-containing protein 1 (PDZK1) and that disruption of this interaction substantially impairs prostacyclin mediated endothelial cell migration and *in vitro* angiogenesis [26].

Hence, there have been significant advances in knowledge of the complex mechanisms of signalling and regulation of the hIP which have, in turn, greatly advanced understanding of the protective role of prostacyclin and of the hIP within the vasculature including of its role in promoting angiogenesis and/or vascular repair in response to injury [4, 5, 14]. Furthermore, recent genome-association studies have provided additional evidence of their functional importance within the vasculature. For example, several single nucleotide polymorphisms (SNPs) have been identified within the coding sequence of the hIP that correlate with predisposition to cardiovascular disease (CVD) including enhanced intimal hyperplasia and platelet activation in deep vein thrombosis in individuals carrying the synonymous V53V/S328S and non-synonymous R212C mutations, respectively [27, 28]. More recently, 3 additional dysfunctional non-synonymous SNPs were identified within the hIP and the occurrence of major coronary artery obstruction is significantly elevated in CAD subjects carrying any of those dysfunctional hIP variants [29]. While SNPs have also been identified in the 5' flanking region of the hIP gene (PTGIR) [30], as the regulatory promoter of the hIP gene remains relatively uncharacterized, however, it is currently unknown whether such SNPs may also contribute to population variations in hIP expression levels and/or to predisposition to CVD/CAD.

Through recent studies, we have initiated a series of investigations to obtain a greater understanding of the factors that regulate expression of the hIP gene in cells derived from the human vasculature, including in the megakaryoblastic human erythroleukemia (HEL) 92.1.7 cell line as well as in vascular endothelial and aortic smooth muscle cells [15, 31]. Through one of those studies, we established that hIP gene expression is under the basal transcriptional regulation of Sp1, PU.1 and Oct-1 through their binding to *cis*-acting elements within the proximal core promoter [31]. In that same study, a major upstream repressor region (URR) was also identified but remained to be characterized. Hence, a central aim of this study was to characterize the URR identified within the hIP regulatory promoter, herein termed the PrmIP, seeking to identify the *cis*-acting elements and *trans*-acting factors that regulate transcriptional repression of the hIP gene in HEL cells.

The pluripotent HEL cell line is frequently employed as an early megakaryoblastic model and can be induced to undergo differentiation toward the platelet progenitor megakaryocytic phenotype by cytokines, growth factors and phorbol esters, such as phorbol 12-myristate 13-acetate (PMA) [32]. Hence, given the critical role of prostacyclin-mediated signalling in platelets, the current study also sought to investigate the influence of phorbol ester-induced megakaryocytic differentiation of HEL cells on hIP gene expression. Herein, we have uncovered a novel mechanism of transcriptional repression and PMA-induction of PrmIP-directed gene expression that occurs through the regulated binding of C/EBPδ and PU.1 to the URR and of Sp1, PU.1 and Oct-1 to the core promoter region, respectively. These studies greatly advance understanding of the mechanisms of regulation of the hIP gene within the vasculature, including during megakaryocytic differentiation of the model platelet progenitor HEL cell line.

2. MATERIALS AND METHODS

2.1. Materials

Dual Luciferase® Reporter Assay System, pGL3Basic (PGL3B) and pRL-Thymidine Kinase (pRL-TK) were from Promega. DMRIE-C®, RPMI 1640 culture media and fetal bovine serum (FBS) were from Invitrogen. *Anti*-C/EBPβ (sc-150 X), *anti*-C/EBPδ (sc-636 X), *anti*-Sp1 (sc-59 X), *anti*-PU.1 (sc-22805 X), *anti*-Oct-1 (sc-232 X), normal rabbit IgG (sc-2027), goat *anti*-rabbit horseradish peroxidase (sc-2004) and mouse *anti*-goat horseradish peroxidase (sc-2354) were from Santa Cruz biotechnology. *Anti*-HDJ-2 (MS225 P1ABX) antibody was from Neomarkers.

2.2. Construction of luciferase-based genetic reporter plasmids

The plasmid pGL3B:PrmIP, encoding PrmIP (nucleotides -2449 to -772, relative to the translational start codon at +1) from the human IP gene in the pGL3B reporter vector, in addition to pGL3B:PrmIP1, pGL3B:PrmIP2, pGL3B:PrmIP3, pGL3B:PrmIP4, pGL3B:PrmIP5, pGL3B:PrmIP6 and pGL3B:PrmIP7 were previously described [31].

2.3. Site-directed Mutagenesis

Site-directed mutagenesis (SDM) was carried out using the Quik-Change™ method (Agilent). The identities of the PrmIP elements subjected to SDM, with their starting positions in brackets, the nucleotides that were changed in underlined bold, templates used and names of the corresponding plasmids generated, as well as the identity, sequence and corresponding nucleotides of the specific primers used are listed below.

1. p53 (-1472), from ggCATGTct to ggCAT**AC**ct using template pGL3B:PrmIP4 to generate pGL3B:PrmIP4^{p53*}. Primers Kin 756 (5'-CAGGCTCGAGGGACTGGCAT**AC**CTCTCTCTGGCCAAGC - 3') and complementary Kin 757.
2. PU.1 (-1454), from ccTTCCtc to ccTT**T**Ctc using template pGL3B:PrmIP4 to generate pGL3B:PrmIP4$^{PU.1(a)*}$. Primers Kin887 (5'-CTGGCCAAGCCTCCTT**T**CTCAGCTTTCTGGAAG-3') and complementary Kin888.
3. STAT (-1433), from ctGGAAgg to ct**A**G**C**Agg using template pGL3B:PrmIP4 to generate pGL3B:PrmIP4^{STAT*}. Primers Kin837 (5'-CTCCTTCCTCAGCTTTCT**A**G**C**AGGAGTGAATTGTGTC -3') and complementary Kin838.
4. PU.1 (-1375), from gaGGAAtt to gaGG**G**Att using template pGL3B:PrmIP4 to generate pGL3B:PrmIP4$^{PU.1(b)*}$, and using template pGL3B:PrmIP4$^{PU.1(a)*}$ to generate pGL3B:PrmIP4$^{PU.1(a,b)*}$. Primers Kin889 (5'-CACTACATCAGAGAGG**G**ATTTCCTGGTCATTTC -3') and complementary Kin890.
5. Nrf1 (-1356), from tgGTCATtt to tgGT**TG**Ttt using template pGL3B:PrmIP4 to generate pGL3B:PrmIP4^{Nrf1*}. Primers Kin833 (5'-CAGAGAGGAATTTCCTGGT**TG**TTTCTCAATCCCTGGGC-3') and complementary Kin834.
6. NFκB (-1359), from gaGGAATTTCCtg to gaGGA**C**TTTCCtg using template pGL3B:PrmIP4 to generate pGL3B:PrmIP4$^{NFκB(a)*}$. Primers Kin655 (5' - CACTACATCAGAGAGGA**C**TTTCCTGGTCATTTCTC - 3') and complementary Kin656.
7. NFκB (-1363), from gaGGAATTTCCtg to gaGGAAT**C**TCCtg using template pGL3B:PrmIP4 to generate pGL3B:PrmIP4$^{NFκB(b)*}$. Primers Kin657 (5' - CACTACATCAGAGAGGAAT**C**TCCTGGTCATTTCTC - 3') and complementary Kin658.
8. C/EBP (-1358), from tcTCAAtc to tcTCA**C**tc using template pGL3B:PrmIP4 to generate pGL3B:PrmIP4$^{C/EBP*}$, using template pGL3B:PrmIP4$^{PU.1(a)*}$ to generate pGL3B:PrmIP4$^{PU.1(a)*,C/EBP*}$ and using template pGL3B:PrmIP4$^{PU.1(b)*}$ to generate pGL3B:PrmIP4$^{PU.1(b)*,C/EBP*}$. Primers Kin891 (5'-CCTGGTCATTTCTCA**C**TCCCTGGGCAATGT-3') and complementary Kin892.
9. C-LH (-1300), from gaATAGATcc to gaATA**TC**Tcc using template pGL3B:PrmIP4 to generate pGL3B:PrmIP4^{C-LH*}. Primers Kin831 (5'-GGGCCTGGAGCCCAGAATA**TC**TCCCAGAGGCCACCCTGAGACAG -3') and complementary Kin832.

The plasmids pGL3B:PrmIP6^{Sp1*}, pGL3B:PrmIP6$^{PU.1*}$, pGL3B:PrmIP6^{Oct-1*}, pGL3B:PrmIP6$^{Sp1*,PU.1*}$, pGL3B:PrmIP6$^{Sp1*,Oct-1*}$, pGL3B:PrmIP6$^{PU.1*,Oct-1*}$ and pGL3B:PrmIP6$^{Sp1*,PU.1*,Oct-1*}$ were previously described [31].

2.4. Cell Culture

Human erythroleukemic (HEL) 92.1.7 cells, obtained from the American Type Culture Collection, were cultured in RPMI 1640, 10 % FBS. Cells were grown at 37 ^{o}C in a humid environment with 5 % CO_2 and were confirmed to be free of mycoplasma contamination.

2.5. Luciferase-based Genetic Reporter Assays

Human erythroleukemic (HEL) 92.1.7 cells were co-transfected with the various pGL3B-recombinant plasmids, encoding firefly luciferase, along with pRL-TK, encoding renilla luciferase, using DMRIE-C® transfection reagent as previously described [33]. In the case of PMA treatments, the medium was supplemented with PMA (100 nM) or, as a control, with vehicle (0.1% (v/v) DMSO) ~24 h post-transfection and cells were incubated for a further 24 h before harvesting. Cells were then assayed for firefly and renilla luciferase activities using the Dual-Luciferase Reporter Assay System^{TM}, and luciferase activities were calculated as a ratio (firefly:renilla luciferase) and expressed in relative luciferase units (RLU) [33].

To investigate the effect of over-expression of C/EBPβ, C/EBPδ and PU.1 on PrmIP-directed gene expression, HEL cells were co-transfected with pGL3B:PrmIP4 (1.5μg) and 30ng of pRL-TK along with either pCMV5:C/EBPβ, pCMV5:C/EBPδ or pCMV5:PU.1 or, as a control, pCMV5 (1μg). Cells were harvested 48 h post-transfection and assayed for luciferase activity, as described before. pCMV5:C/EBPβ, encoding the full length cDNA for C/EBPβ was obtained from ImaGenes (Clone IMAGp998D1710064Q). pCMV5:PU.1, encoding full length PU.1 was from GeneService LTD (Clone number 5210783). pCMV5:C/EBPδ [34] was generously donated by Professor A-Mei Huang, Kaohsiung Medical University (Kaohsiung, Taiwan).

A gene reporter assay was performed to investigate changes in intracellular cAMP levels in response to stimulation of the hIP with its selective agonist cicaprost, using the method previously described[15]. In brief, the medium was supplemented with PMA (100 nM), or, as a control, with vehicle (0.1% (v/v) DMSO) ~24 h post-transfection. Cells were treated 48 h after transfection with IBMX (100 μM) at 37 °C for 30 min and then stimulated with either vehicle (V; DMSO) or 1 μM cicaprost at 37 °C for 3 h before harvesting. Firefly and *Renilla* luciferase activities were assayed 52 h after transfection using the Dual Luciferase Assay System® and expressed as a ratio (RLU).

2.6. Real-time PCR analysis:

Total RNA was isolated using TRIzol reagent (Invitrogen) from HEL cells (5 x 10^6 approximately). In the case of PMA treatment, cells were preincubated for 24h with PMA (100 nM) or, as a control, with vehicle [0.1% (v / v) DMSO]. DNase I-treated total RNA was converted to first-strand (1°) DNA with M-MLV reverse transcriptase (Promega). Real-time quantitative (QT) -PCR analysis was then performed, using the SyBr green reaction kit (Promega), with primers designed to specifically amplify hIP mRNA sequences (forward, 5'- GAAGGCACAGACGCACGGGA-3', Nu -57 to -37 of Exon 1; Kin264; reverse, 5'-GGCGAAGGCGAAGGCATCGC -3'; Nu 294 to 275 of Exon 2; Kin266) to generate a 348 bp amplicon or, as an internal control, using primers designed to amplify a 588bp region of the human 18s rRNA gene (forward, 5'-CGGCTACCACATCCAAGGAA-3'; reverse, 5'-TCGTCTTCGAACCTCCGACT-3'). The levels of hIP mRNA were normalized using corresponding 18s rRNA expression levels, to obtain Ct values. Relative IP mRNA expression levels were then calculated using the formula $2^{-\Delta\Delta Ct}$ [35], and data is presented as mean changes in hIP mRNA expression in over-expressed or PMA-treated cells relative to those levels in control transfected (pCMV5) or vehicle-treated (0.1% (v / v) DMSO) cells, set to a value of 1 (Relative expression ± SEM, n = 3).

2.7. Immunoblot Analysis

Detection of endogenous or ectopically expressed C/EBPβ, C/EBPδ, PU.1, Sp1 and Oct-1 proteins in HEL cells was confirmed by immunoblot analysis. Briefly, whole cell protein from HEL cells or HEL cells transiently co-transfected with pCMV5:C/EBPβ, pCMV5:C/EBPδ or pCMV5:PU.1 or, as a control, with pCMV5 (50μg per lane) were resolved by SDS-PAGE (10 % acrylamide gels) and transferred to polyvinylidene difluoride (PVDF) membrane according to standard methodology. Membranes were screened using *anti*-C/EBPβ, *anti*-C/EBPδ, *anti*-PU.1, *anti*-Sp1 and *anti*-Oct-1 sera in 5 % non-fat dried milk in 1 x TBS (0.01 M Tris-HCl, 0.1 M NaCl) overnight at 4°C followed by washing and screening using either goat *anti*-rabbit horseradish peroxidise (sc-2004) or mouse *anti*-goat horseradish peroxidise (sc-2354) followed by chemiluminescence detection. To confirm uniform protein loading in each case, the blots were stripped and rescreened with *anti*-HDJ-2 antibody (Neomarkers) to detect endogenous HDJ-2 protein expression which served as an additional protein loading control.

2.8. Chromatin Immunoprecipitation (ChIP) Assays

ChIP assays were performed in HEL cells as previously described [36]. Briefly, HEL cells (1 x 10^8) were grown in RPMI, 10 % FBS to 70 % confluency and collected by centrifugation at 2,000 g for 5 min at 4 ^oC, washed twice in ice-cold PBS and resuspended in 50 ml serum-free RPMI. For PMA treatments, cells were pre-incubated with PMA (100 nM for 0, 5, 8, 16 and 24 h). Formaldehyde (1 %)-cross linked chromatin was sonicated to generate fragments ranging from 350 bp to 1000 bp in size, as illustrated in Supplemental Fig. 1A). Sheared chromatin was resuspended in a final volume of 6 ml lysis buffer. Prior to immunoprecipitation, chromatin was incubated with 40 µg normal rabbit IgG overnight at 4 ^oC on a rotisserie, after which 250 µl of salmon sperm DNA/protein A agarose beads (Millipore) were added and chromatin was precleared overnight at 4 ^oC with rotation. Thereafter, for chromatin immunoprecipitation (ChIP) assays, aliquots (672 µl) of the precleared chromatin were incubated with *anti*-C/EBPβ, *anti*-C/EBPδ *anti*-PU.1, *anti*-Sp1, *anti*-Oct-1 (10 µg aliquots in all cases) or, as controls, with normal rabbit IgG (10 µg) antibodies or in the absence of primary (1°) antibody (-AB). Aliquots (270 µl) were stored for use as input chromatin DNA. All antibodies used for ChIP analysis were ChIP validated by the supplier (Santa Cruz) and have been used previously for such analyses [31, 36-40]. Following elution of the immune complexes from the beads, formaldehyde cross-links were reversed by incubation at 65 ^oC overnight followed by protease digestion with proteinase K (Gibco-BRL #25530-031; 9 µl of 10 mg/ml) at 45 ^oC for 7 h. After precipitation, samples were resuspended in 50 µl dH_2O. PCR analysis was carried out using 2-3 µl of ChIP sample as template or, as a positive control, with an equivalent volume of a 1:4 dilution of the input chromatin DNA. The identities of the primers used for the ChIP PCR reactions, as well as their sequences and corresponding nucleotides within PrmIP are listed below.

1. Kin 1286: 5'-TCGGGTCTCTGCAGGGTGAGCTGGGTGC- 3', Nu -1556 to -1528
2. Kin 1287: 5'- GCCTGGGCTGTCTCAGGGTGGCCTCTGG -3', Nu -1327 to -1299
3. Kin538: 5'-GAGA GGTACC ACCCTGAGACAGCCCAGG-3', Nu -1291 to -1263
4. Kin274: 5'-CTCTCAAGCTTCTCTCCAGTCTTGCCCAGGCTC -3' , Nu -827 to -794
5. Kin 534: 5'- GAGAGGTACCCAGCGGTGGTGGCTTGGCTGTG -3' , Nu -1783 to -1761
6. Kin 677: 5'-CTCTAAGCTTGGAGACTTCCATGGC -3' , Nu -1577 to -1562
7. Kin 364: 5'- TTGGGTCCAGAAGGTCGAGGC3 -3', Nu -1081 to -1061
8. Kin 365: 5'- GCGAACCAGGGCGAGGC -3' , Nu -711 to -695

For quantitation of the relative abundance of the PCR products derived from the individual test or control immunoprecipitates relative to that of the products derived from the respective input chromatins, real-time QT-PCR reactions were carried out for the same number of cycles (typically 35 cycles) using the Agilent MX3005P QPCR system to obtain cycle threshold (Ct) values. Changes in relative PCR product intensities were then calculated using the Relative Quantification method using the formula $2^{-\Delta\Delta Ct}$ [35]. Data is presented as mean product intensities of the individual test or control immunoprecipitates expressed as a percentage relative to those derived from the corresponding input chromatins. For all ChIP-based experiments, PCR (semi-quantitative and real time QT-PCR) data presented is obtained from at least 3 independent ChIP immunoprecipitations using chromatin extracted on at least 3 occasions, rather than from triplicate PCRs using chromatin precipitated from single ChIP experiments.

2.9. Statistical analysis

Statistical analyses of differences were carried out using the unpaired Student's *t* test or two-way ANOVA followed by post hoc Dunnett's multiple comparison *t* tests, employing GraphPad Prism, version 4.00 package. All values are expressed as mean ± standard error of the mean (SEM). P- values of less than or equal to 0.05 were considered to indicate a statistically significant difference. To investigate overall differences between time-dependent increases in PrmIP- and PrmIP4-directed luciferase expression, nonlinear regression (R^2) and *F*-test analyses were carried out, where P-values of the slopes were greater than 0.05 and considered not to indicate a statistically significant difference. As relevant, *, **, *** and **** indicate $p \leq 0.05$, 0.01, 0.001 and 0.0001, respectively.

3. RESULTS:

3.1. Identification of an upstream repressor region (URR) within PrmIP

Prostacyclin primarily signals through its specific cell surface prostacyclin receptor, or IP, and plays a central role in haemostasis and in vascular repair [1, 2, 4, 5, 13, 14]. In humans, expression of the hIP is under the control of its regulatory promoter, herein referred to as the PrmIP and defined as nucleotides -2449 to -772 located upstream of the translation initiation codon within the hIP gene (Fig 1A). In recent studies aimed at identifying the factors that regulate hIP gene expression within the vasculature, including in the model megakaryoblastic HEL 92.1.7 cell line, it was established that its expression is transcriptionally regulated by Sp1, PU.1 and Oct-1 through their binding to *cis*-acting elements within the core PrmIP region at -1042 to -917 [31], as illustrated in Fig 8A. In a follow up study, it was also established that hIP gene expression is directly regulated by estrogen through a transcriptional mechanism involving the direct binding of the estrogen receptor (ER) □, but not ER□, to a highly conserved upstream estrogen response element (ERE) located at approximately -1676 [15] (Fig 8A). While the former study also revealed an upstream repressor region (URR) within PrmIP, between -1524 to -1293, the identity of the *cis*-acting elements or *trans*-acting factors that regulate the URR remain to be investigated [31]. Hence, the initial aim of the current study was to further investigate the factors regulating hIP gene expression in HEL cells by identifying the *trans*-acting factors that bind and regulate the URR within PrmIP.

Initially, and consistent with previous findings [31], 5' deletional analysis and luciferase-based genetic reporter assays confirmed the presence of the URR located between -1524 to -1293 within PrmIP (Fig 1A). Specifically, 5' deletion of nucleotides from PrmIP4 (-1524) to generate PrmIP5 (-1293) yielded a 1.7-fold increase in luciferase expression ($P < 0.0001$). Bioinfomatic analysis of PrmIP [41] predicted several *cis*-acting elements within the putative URR, including 2 PU.1 binding sites, designated PU.1(a) and PU.1(b) at -1454 and -1375, respectively, and a C/EBP site at -1358 (Fig 1B). Site-directed mutagenesis (SDM) in conjunction with genetic reporter assays established that disruption of the PU.1(b) and C/EBP sites individually led to 1.4- and 1.3-fold increases in PrmIP-directed luciferase activity ($P = 0.0003$ and $P = 0.0004$) respectively, while mutation of the PU.1(a) site yielded a more subtle, yet significant, increase (1.2-fold; $P = 0.0065$). On the other hand, SDM of the various other predicted elements within the putative URR did not significantly affect PrmIP-directed luciferase expression (Fig 1B).

Combined disruption of the PU.1(a) and PU.1(b) sites resulted in a 1.4-fold increase in PrmIP4-induced luciferase expression ($P = 0.0002$), to levels not substantially greater than disruption of the PU.1(b) site alone. On the other hand, disruption of the PU.1(b) and C/EBP elements together almost completely alleviated repression resulting in a 1.6-fold increase ($P < 0.0001$) in PrmIP4-directed luciferase expression to levels that were not substantially different to those of PrmIP5 ($P = 0.0946$). It was notable that there was no significant difference between the effect of combined disruption of the PU.1(b) and C/EBP elements relative to disruption of all PU.1(a), PU.1(b) and C/EBP elements together ($P = 0.9559$). Furthermore, combined disruption of the PU.1(a) and C/EBP elements did not substantially affect PrmIP4-directed luciferase expression relative to mutating the C/EBP element alone ($P = 0.1015$). Taken together, these data have identified a major URR within PrmIP and established that repression in this region is largely mediated by transcription factor binding to the putative PU.1(b) and C/EBP elements at -1375 and -1358, respectively, but that the PU.1(a) element at -1454 may only play a minor role, if any.

3.2. Characterisation of functional PU.1 and C/EBP *cis*-acting elements within the URR

The CCAAT/enhancer binding proteins (C/EBPs) are a family of 6 transcription factors (C/EBP□ – C/EBPP□) containing a highly conserved C-terminal basic leucine zipper (bZIP) domain involved in dimerization and DNA binding [42], where C/EBPβ and C/EBPδ regulate transcription of a number of CV-associated genes, including COX-2, peroxisome proliferator-activated receptor ϒ and platelet-derived growth factor-α receptor [43-46]. PU.1, a transcription factor essential for hematopoietic development, has been previously confirmed to be the only member of the Ets family to bind to the core region of PrmIP to regulate basal hIP gene expression [31]. Hence, to investigate if PU.1, C/EBPβ and/or C/EBPδ actually bind to the URR of the PrmIP *in vivo*, chromatin immunoprecipitation (ChIP) assays were carried out using chromatin extracted from HEL cells and antibodies specific to endogenous PU.1, C/EBPβ and C/EBPδ. In general, the fragment size of the sheared chromatin DNA used in the ChIP studies ranged from 350 – 1000 bp and, for all ChIP studies, PCR amplicons generated from immune-precipitated chromatin DNA were analysed by agarose gel electrophoresis (e.g Fig 2A & 2B) and by real-time quantitative PCR (e.g Fig 2C).

PCR analysis using primers specific to the -1528 to -1327 region of PrmIP generated amplicons from the *anti*-C/EBPδ and, to a lesser extent, from the *anti*-PU.1 immunoprecipitates (Fig 2A & 2C(i)). Specific amplicons were also generated from the input chromatin, but not from the *anti*-C/EBPβ or the normal rabbit

immunoglobulin G (IgG) immunoprecipitates or the no primary (1^o) antibody control (-AB) ChIP assays (Fig 2A & 2C(i)). As an additional control of the specificity of C/EBPδ and PU.1 binding to the URR, PCR analysis using primers specific to an upstream region of PrmIP, spanning -1761 to -1577, generated amplicons from the input chromatin but not from the *anti*-C/EBPβ, *anti*-C/EBPδ, *anti*-PU.1, IgG immunoprecipitates or the no 1^o antibody controls, as illustrated by agarose gel electrophoresis data (Fig 2B). However, Real-time QT-PCR analysis of this data indicates that products were generated from *anti*-C/EBPβ, *anti*-C/EBPδ and *anti*-PU.1 immunoprecipitates in the -1761 to -1577 region, but their relative abundance is substantially reduced relative to those products derived from the -1528 to -1327 region (Fig 2C(ii)). As a further negative control, QT-PCR analysis using primers which were previously described by us [47] and are specific to a region of Prm3 of the thromboxane receptor (TP) gene generated amplicons from the input chromatin but not from the *anti*-C/EBPβ, *anti*-C/EBPδ, *anti*-PU.1, IgG immunoprecipitates or the no 1^o antibody control (Supplemental Fig 1B(i)). Endogenous expression of C/EBPβ, C/EBPδ and PU.1 in HEL cells was confirmed by immunoblot analysis, where secondary immunoblotting for the ubiquitously expressed HDJ-2 confirmed uniform protein loading (Fig 2D (i-iii)). Noteworthy, 3 separate forms of C/EBPβ referred to as LAP1 (46 kDA), LAP2 (41 kDa) and LIP (20 kDa) forms [42] were detected in HEL cells where the LIP form containing only the bZIP domain was the most abundant (Fig 2D (i)).

To further examine the possible role of C/EBPβ, C/EBPδ and PU.1 in the transcriptional regulation of PrmIP, the effect of their ectopic expression on hIP mRNA and PrmIP-directed reporter gene expression was investigated. Quantitative (QT) -PCR analysis confirmed that ectopic expression of C/EBPβ had no significant effect on hIP mRNA expression ($P = 0.24$), whereas C/EBPδ reduced ($P = 0.013$) and PU.1 increased ($P = 0.03$) its expression (Fig 3A). Similarly, ectopic expression of C/EBPβ did not significantly affect PrmIP-directed luciferase expression ($P = 0.125$), whereas C/EBPδ reduced ($P < 0.0001$) and PU.1 increased ($P = 0.0009$) its expression (Fig 3B). In all cases, immunoblot analysis confirmed over-expression of C/EBPβ, C/EBPδ and PU.1 in the transfected HEL cells (Fig 3C (i-iii)).

Taken together, these data identify PU.1(b) and C/EBP as the critical *cis*-acting elements within the URR which mediate repression of PrmIP in HEL cells. ChIP data established that C/EBPδ, but not C/EBPβ, and to a lesser extent PU.1, binds within the URR of PrmIP *in vivo*. Furthermore, it was established that ectopic expression of C/EBPδ and PU.1 negatively and positively regulate hIP mRNA and gene expression, respectively, while C/EBPβ had no effect. Overall, it is proposed that along with C/EBPδ, PU.1 negatively regulates PrmIP transcription within the URR where PU.1(b) at -1375 and C/EBP at -1358 are the main *cis*-acting elements involved.

3.3. Effect of PMA on IP expression in HEL cells: Identification of PMA-responsive region (PRR) 1 and PRR2 within PrmIP

It was also sought to investigate the influence of megakaryocyte differentiation on hIP gene expression following exposure of HEL cells to the phorbol ester PMA and, thereafter, to potentially identify the critical PMA responsive *cis*-acting element(s) within PrmIP. QT-PCR and luciferase-based gene reporter analyses established that PMA treatment (100 nM, 24 hr) significantly up-regulated IP mRNA expression ($P = 0.0006$; Fig 4A) and PrmIP-directed luciferase expression ($P \leq 0.0001$; Fig 4B (i)) but had no effect on pGL3B-directed luciferase expression ($P = 0.79$; Fig 4B (ii)). As stated, the hIP is primarily coupled to Gs-mediated adenylyl cyclase activation leading to agonist-dependent increases in cAMP generation [1, 10]. Thus, the effect of PMA treatment on the functional expression of the hIP in HEL cells was investigated by examining its effect on agonist-induced cAMP generation where cicaprost was used as the IP selective agonist. While stimulation of HEL cells with cicaprost led to a 2-fold increase in cAMP generation in vehicle -treated cells (0.1 % DMSO, 24 hr; $P < 0.0001$), pre-incubation of cells with PMA (100nM, 24 hr) resulted in a 6.24-fold increase in cAMP generation ($P < 0.0001$; Fig 4C).

Thereafter, 5' deletional analysis and genetic reporter assays were used to localize the main PMA-responsive regions within PrmIP (Fig 5A & 5B). Pre-incubation of HEL cells with PMA resulted in a 1.85-fold increase in PrmIP-directed luciferase expression ($P \leq 0.0001$). Levels of PMA-induced luciferase expression directed by the successive 5' deletion subfragments PrmIP1 – PrmIP4 were not significantly different to that of PrmIP (Fig 5A & 5B). However, 5' deletion of nucleotides from PrmIP4 (-1524) to generate PrmIP5 (-1293) reduced the level of PMA-induced luciferase expression from 1.85-fold to 1.5-fold ($P = 0.0002$). While further 5' deletion of PrmIP5 (-1293) to PrmIP6 (-1042) had no effect on the PMA-induction, deletion of PrmIP6 to generate PrmIP7 (-917) almost completely abolished the PMA- induction (1.07-fold; P-value < 0.0001; Fig 5A & 5B). These data establish that there are 2 PMA-responsive regions (PRRs) within PrmIP, where PRR1 is located between the subfragments PrmIP4 and PrmIP5 (-1524 to -1293) while PRR2 is between PrmIP6 and PrmIP7 (-1042 to -917) within the core promoter region [31]. To

further validate that the main PMA responsive regions PRR1 and PRR2 are indeed localized downstream/3' of PrmIP4, the time course of PMA-induced luciferase reporter gene expression directed by PrmIP4 was compared with that directed by PrmIP (Fig 5C & 5D). There was no significant difference between PMA-induced upregulation of PrmIP- and PrmIP4-directed luciferase expression (F-test analysis, P = 0.7007), confirming that all of the PMA responsive regions are found within PrmIP4.

3.4. Identification of the *cis*-acting PMA responsive elements within PRR1

As stated, the initial studies herein have established that hIP gene expression is subject to transcriptional repression through the binding of PU.1 and C/EBPδ to the PU.1(b) and C/EBP *cis*-acting elements of the URR identified between PrmIP4 (-1524) and PrmIP5 (-1293). Furthermore, it has also been established that the PRR1 also maps to the same region between PrmIP4 and PrmIP5. Hence, to further localize and/or identify the main *cis*-acting elements that mediate the PMA-responsive effect within PRR1, the effect of PMA-induced luciferase expression directed by the previously described mutated derivatives of PrmIP4 (Fig 1B & 1C) were compared with that of wild type PrmIP4 (Fig 6A & 6B; Supplemental Fig 2A & 2B). As previous, while PMA treatment led to a 1.85-fold increase in PrmIP4-directed luciferase expression, specific mutation of the PU.1(a) and PU.1(b) elements, but not of the C/EBP or other putative *cis*-acting elements, within the overlapping PRR1/URR reduced the level of PMA-induction (Fig 6A & 6B; Supplemental Fig 2A & 2B). More specifically, mutation of the PU.1(a) and PU.1(b) elements within PrmIP4 either individually (P = 0.0075 and P = 0.008, respectively) or collectively (P = 0.0005) reduced the PMA-induction from 1.85-fold to approximately 1.5-fold, while disruption of the C/EBP element either alone (P = 0.82) or in various combinations had no significant effect (Fig 6A & 6B). In fact, levels of PMA-induced luciferase expression by PrmIP4 carrying the mutated PU.1(a) or PU.1(b) elements, either alone or in combination, were not significantly different to those levels induced by the PrmIP5 subfragment which does not contain the PRR1 (P = 0.31). Collectively, these data establish that the PU.1(a) and PU.1(b) elements are the critical PMA-responsive *cis*-acting elements within PRR1. Furthermore, since the effect of disruption of the PU.1(a) and PU.1(b) elements alone was similar to their combined disruption, the data also suggests that binding of PU.1 at one of the sites (e.g to PU.1(a)) may depend on binding at the other site (e.g to PU.1(b)) or *vice versa*.

To investigate transcription factor binding to the over-lapping URR/PRR1 regions *in vivo*, as previous (Fig 2A), ChIP analyses were carried out using antibodies directed to endogenous C/EBPβ, C/EBPδ and PU.1 and chromatin extracted from HEL cells following treatment with PMA for 0 - 24 hr (0, 5, 10, 16 and 24 hr). Amplicons generated were either analysed by agarose gel electrophoresis (Fig 6C & Fig 6D) or by real-time quantitative (QT) PCR (Fig 6E(i-v) & Fig 6F(i & ii)). As expected, in all cases, primers surrounding the URR/PRR1 region generated amplicons from the input chromatin but not from *anti*-C/EBPβ immunoprecipitates or from the control assays (IgG immunoprecipitates or the no 1^{o} antibody control; Fig 6C & Fig 6E(i)). Additionally, and consistent with previous data (Fig 2A), at 0 hr, amplicons were generated from the *anti*-C/EBPδ immunoprecipitate and to a lesser extent from the *anti*-PU.1 immunoprecipitate. In contrast, at 5 hr, the relative abundance of the PRR1 amplicon generated from the *anti*-PU.1 immunoprecipitate was substantially increased while that from the *anti*-C/EBPδ immunoprecipitate was greatly diminished (Fig 6C & Fig 6E(ii)). At 10 hr, a PRR1 amplicon was generated from the *anti*-PU.1, but not from the *anti*-C/EBPδ immunoprecipitate and this pattern was sustained at 16 hr and 24 hr post-PMA treatment (Fig 6C & 6E(iii-v)). As an additional control for specificity, PCR analysis using primers specific to an upstream region of PrmIP, spanning -1761 to -1577, generated an amplicon from the input chromatin but not from the *anti*-C/EBPβ, *anti*-C/EBPδ, *anti*-PU.1 immunoprecipitates or the control ChIP assays regardless of the absence (0 hr) or presence (24hr) of PMA, as indicated by the agarose gel electrophoresis data (Fig 6D). As previous, real-time QT-PCR analysis of this data indicates that products were generated from *anti*-C/EBPβ, *anti*-C/EBPδ and *anti*-PU.1 immunoprecipitates in the -1761 to -1577 region, but their relative abundance is substantially reduced relative to products derived from the -1528 to -1327 region, in the absence or presence of PMA (Fig 6F(i & ii)). Also as previous, as a further negative control, QT-PCR analysis using primers specific to a region of Prm3 of the TP gene [47] generated amplicons from the input chromatin but not from the *anti*-C/EBPβ, *anti*-C/EBPδ, *anti*-PU.1, IgG immunoprecipitates or the no 1^{o} antibody controls (Supplemental Fig 1B(i & ii)). In parallel with this, immunoblot analysis established that while the level of PU.1 expression in HEL cells was not altered following PMA treatment, the actual level of C/EBPδ expression was substantially reduced at 16 and 24 hr post-incubation (Fig 6G & 6H), while immunoblotting for the ubiquitously expressed HDJ-2 confirmed uniform protein loading (Fig 6I).

Collectively, these data establish that PU.1(a) and PU.1(b) are the critical *cis*-acting elements which contribute to the PMA-induction of hIP gene expression through the over-lapping URR/PRR1 identified

herein within PrmIP. Additionally, through ChIP analyses it was established that under basal conditions, in the absence of PMA-induced HEL cell differentiation, C/EBPδ and to a lesser extent PU.1 bind to mediate repression of PrmIP-directed gene expression. However, in response to PMA induction of PrmIP-directed transcriptional expression, there is an overall switch from predominant C/EBPδ to PU.1 binding in this region, thereby converting the URR to a PRR1, which also coincides with a reduction in C/EBPδ protein expression whilst the level of PU.1 protein expression remains relatively unchanged.

3.5. Identification of the *cis*-acting PMA responsive elements within PRR2

As stated, it has been previously established that hIP gene expression is under basal regulation through the binding of Sp1, PU.1 and Oct-1 to functionally active *cis*-acting elements within the core promoter region (-1042 to -917) of PrmIP [31]. Furthermore, data herein also establish that the second PMA responsive region (PRR2) is also localized to this region (Fig 5A & 5B). Hence, it was hypothesised that the Sp1, PU.1 and Oct-1 elements within the core promoter/PRR2 regions may contribute to the PMA-induced increase in PrmIP-directed gene expression. Treatment of HEL cells with PMA led to a 1.5-fold increase in PrmIP6-directed luciferase reporter gene expression (Fig 7A & 7B). While mutation of the Sp1, PU.1 and Oct-1 elements individually did not substantially affect the PMA- induction of PrmIP6 ($P = 0.39$, $P = 0.96$ and $P = 0.41$, respectively), disruption of all 3 elements together ($P = 0.0004$) and/or in certain double combinations only (Sp1 & Oct-1, $P = 0.0041$; PU.1 & Oct-1, $P = 0.0044$) almost completely abolished that induction (Fig 7A & 7B). Moreover, levels of PMA-induced luciferase expression directed by PrmIP6 carrying the mutated Sp1, PU.1 and Oct-1 elements in combination, were not significantly different to those levels directed by the PrmIP7 subfragment which does not contain the PRR2 ($P = 0.1506$).

Thereafter, ChIP analysis was used to investigate Sp1, PU.1 and Oct-1 binding to the PRR2 region of PrmIP *in vivo* following PMA-induced differentiation of HEL cells over a 0 – 24 hr period (0, 5, 16 and 24 hr). As previous [31], in the absence of PMA-treatment, primers surrounding the PRR2 region of PrmIP generated amplicons from the input chromatin and from the Sp1, PU.1 and Oct-1 immunoprecipitates but no PRR2 amplicons were generated from the control ChIP assays (0 hr; Fig 7C & 7E(i)). Amplicons were also generated at 5, 16 and 24 hr post-PMA treatment, and the abundance of the products generated from the *anti*-Sp1, *anti*-PU.1 and *anti*-Oct-1 immunoprecipitates were relatively unchanged at 5 hr, but were each substantially increased at the latter time points (16 and 24 hr) suggestive of enhanced transcription factor binding to the chromatin *in vivo* in response to PMA-induced differentiation of HEL cells (Fig 7C & 7E(ii-iv)). In contrast, ChIP analysis using PCR primers specific to an upstream region of PrmIP, spanning -1761 to -1577, which is known not to be regulated by Sp1, PU.1 or Oct-1, did not generate amplicons from the *anti*-Sp1, *anti*-PU.1, *anti*-Oct-1 or control immunoprecipitates, regardless of the absence (0 hr) [31] or presence (24 hr) of PMA (Fig 7D & 7F(i & ii)). While we have previously established that the level of Sp1 expression is not affected by PMA-induced differentiation of HEL cells [37], immunoblot analysis herein confirmed that the levels of PU.1 (Fig 6H) and Oct-1 (Fig 7G) expression were also unaltered in response to PMA treatment.

Taken together, these data establish that the PMA-induced enhanced binding of Sp1, PU.1 and Oct-1 to their *cis*-acting elements within the core PrmIP6 region, which overlaps with the PRR2, contributes to the increased hIP gene expression that occurs during PMA-mediated differentiation of megakaryocytic HEL cells.

4. DISCUSSION

Within the vasculature, prostacyclin serves as a potent vasodilator and is the major inhibitory prostanoid in platelet aggregation [1-3]. The actions of prostacyclin generally oppose those of TXA_2 and alterations in the levels of TXA_2 and prostacyclin or of their specific synthases or their receptors (the TP and IP, respectively) have been implicated in a wide range of vascular disorders [4, 6-8]. Recent studies have shed significant new insights into how naturally occurring synonymous and non-synonymous SNPs within the coding sequence of the hIP contribute to propensity to CVD [28, 29, 48]. While SNPs also occur in the flanking regions of the hIP gene [30], it is currently unknown whether SNPs within the hIP promoter may also contribute to population variations in hIP expression levels and/or to predisposition to CVD/CAD. The hIP promoter, herein termed PrmIP, has been defined as the region spanning nucleotides -2449 to -772 within the hIP genomic region, where the core promoter maps to -1042 to -917 and has been previously characterised [31]. That study also identified a major upstream repressor region (URR) between -1524 to -1293 (relative to the translation initiation codon at +1) and the initial aim of the current study was to identify the essential *cis*-acting elements and *trans*-acting factors which regulate PrmIP transcription within this region in the megakaryoblastic HEL 92.1.7 cell line.

Herein, bioinformatic analysis revealed the presence of nine potential *cis*-acting regulatory elements within the putative URR. Of those elements, only two were found to be functionally important within the URR under basal conditions, namely the PU.1(b) and C/EBP elements located at -1375 and -1358, respectively. More specifically in terms of the 2 putative PU.1 elements, as a role for the putative PU.1(a) element was only evident from the single mutational data, it is likely that it is less important than the PU.1(b) element and that binding of PU.1 to only one of the two putative PU.1 elements, namely to the PU.1(b) site, may be required to partner with C/EBPδ bound to the C/EBP element to mediate transcriptional repression. PU.1, encoded by the *Spi1* gene in humans, is a member of the Ets family of transcription factors and has been reported to play a central role in hematopoeisis [49]. The importance of PU.1 in hematopoiesis is highlighted by the fact that deletion of the mouse equivalent of the *Spi1* gene generates null mice with either fetal or perinatal lethality and multiple defects in blood cell development [50, 51]. As stated, PU.1 is the only member of the Ets family to bind within the core region of PrmIP to direct basal expression [31]. Moreover, PU.1 regulates gene expression by binding to canonical ETS motifs or to composite sites via interaction with other transcription factors such as interferon regulatory factor (Irf) 2, Irf4, Irf8, c-Jun and several members of the C/EBP family [52-58]. PU.1 activity can also be antagonized by interaction with members of the GATA family of transcription factors via a mechanism whereby PU.1 and GATA-1 co-exist on DNA to mutually repress gene expression [51]. Additionally, PU.1 can mediate transcriptional activation through interaction with acetyltransferases including CBP and p300 or repression by interacting with the deacetylases HDAC1, mSin3A and MeCP2 [59].

As stated, the C/EBP family of transcription factors is composed of 6 members, C/EBPα through to C/EBPζ [42]. They are so called because they interact with the CCAAT (cytidine-cytidine-adenosine-adenosine-thymidine) box motif found in many, but not all, eukaryotic promoter sequences. C/EBP members bind to DNA as dimers, whereby they homo- or hetero-dimerise via their C-terminal leucine zipper domains, and are abundantly expressed to regulate diverse processes including energy metabolism, innate and adaptive immunity, inflammation, hematopoiesis, adipogenesis, osteoclastogensis, cell cycle, cellular proliferation and differentiation [40, 53, 60-63]. C/EBPβ and C/EBPδ act synergistically to regulate transcription of various genes involved in immune and inflammatory responses [64]. Interestingly, the enzyme COX-2, primarily involved in prostanoid generation in response to inflammation, has been identified as a transcriptional target of both C/EBPβ and C/EBPδ [43]. C/EBPβ, along with cAMP response binding protein (CREB), plays a major role during the initial stage of COX-2 transcriptional activation, while C/EBPδ is subsequently recruited, along with the transcriptional co-activator p300 and several other factors, into a complex which regulates COX-2 transcription [43]. C/EBPβ and C/EBPδ are therefore critical transcriptional regulators of genes involved in prostanoid biosynthesis and function.

Herein, disruption of the PU.1(a), PU.1(b) and C/EBP elements individually within PrmIP led to modest increases in PrmIP4-directed luciferase expression, whereas disruption of the PU.1(b) and C/EBP elements in combination almost completely alleviated repression within the URR region. ChIP analyses indicated that C/EBPδ and to a lesser extent PU.1, but not C/EBPβ, are capable of binding within the URR region. Moreover, ectopic expression of C/EBPδ in HEL cells significantly reduced hIP mRNA and PrmIP-directed gene expression levels whereas, and consistent with previous findings [31], PU.1 significantly increased expression levels while C/EBPβ had no effect. While PU.1 has been shown to positively regulate hIP gene expression through its binding to its *cis*-acting element within the proximal core PrmIP [31], data generated herein suggest that under basal conditions C/EBPδ is predominantly bound to its *cis*-element

within the URR and that it co-operates, or indeed may interact, with PU.1 to repress PrmIP gene expression. In fact, it has long been established that PU.1 can physically interact with C/EBPδ (NF-IL6β) through an interaction dependent on the C-terminal 28 AA residues of PU.1 and that they can simultaneously bind to adjacent DNA binding sites to synergistically influence the basal transcription complex [54].

In light of the data presented herein and from our recent reports characterizing the PrmIP [15, 31], we propose a model to explain the transcriptional regulation of the hIP gene, such as in megakaryocytic HEL cells (Fig 8A). It is proposed that PrmIP contains three spatially distinct regulatory domains; namely the estrogen-responsive region (ERR; -1783 to -1597), the URR described herein (-1524 to -1293) and the core regulatory region (-1042 to -917). In the context of the URR, it is proposed that C/EBPδ binds to its *cis*-acting element and co-operates with PU.1 through its binding to the adjacent PU.1(b) element to repress the basal transcriptional apparatus. Interestingly, multi-sequence alignments confirmed that both the URR region and the PU.1(b) and C/EBP elements themselves are found within the PrmIP promoter regions from a range of other species (Fig 8B), suggesting that this represents an evolutionary conserved mechanism of transcriptional regulation of the hIP gene. It is also noteworthy that the extent of overall identity between the human PrmIP and the IP promoter sequences from all other non-primates is low but that part of the URR, encompassing the PU.1(b) and C/EBP elements, represents the most highly conserved promoter region across all species examined (Fig 8B & data not shown).

As stated, the pluripotent HEL cell line is frequently employed as an early megakaryoblastic model and can be induced to undergo differentiation toward the platelet progenitor megakaryocytic phenotype by a range of agents including phorbol esters [32]. Furthermore, prostacyclin and its analogues have been shown to inhibit the differentiation process [65]. Hence, given the critical *anti*-thrombotic role of prostacyclin in regulating platelet activation status, it was also sought to examine the influence of PMA-mediated megakaryocyte differentiation on hIP gene expression in HEL cells. Data herein demonstrated substantial increases in hIP mRNA and gene expression in response to PMA-induced differentiation. Through deletional analysis, the PMA responsive regions were localised to 2 spatially distinct regions designated PRR1 and PRR2 which were found to co-localize/overlap with the URR and the previously characterized core PrmIP region [31], respectively. Mutational analysis established that binding of PU.1 to the PU.1(a) and PU.1(b) sites, located at -1454 and -1375, respectively, mediates the PMA-induced increase in PrmIP activity within PRR1. Consistent with previous data herein, ChIP analyses reaffirmed that, under basal conditions and in the absence of PMA, C/EBPδ and, to a lesser extent, PU.1, but not C/EBPβ, preferentially bind to the URR/PRR1 region. However, in response to PMA-induction, C/EBPδ was gradually replaced by PU.1 leading to sustained PU.1 binding and transcriptional activation. Coincident with this, immunoblot analysis established that C/EBPδ expression was significantly reduced in a time-dependent manner in response to PMA treatment whilst PU.1 expression was unaffected. Overall, these data suggest that there is a switch in transcriptional regulator binding *in vivo* from predominantly C/EBPδ binding to the URR to predominantly PU.1 binding to the PMA-induced PRR1 region to enhance hIP gene expression and signalling in response to megakaryocyte differentiation. Consistent with this, C/EBPδ has been previously shown to bind to the COX-2 promoter, to regulate COX-2 expression under basal conditions in human foreskin fibroblasts. However, in response to PMA, C/EBPδ expression and binding to the COX-2 promoter were reduced and displaced by C/EBPβ [44]. The observation herein that the overall levels of PU.1 expression were unaltered in response to PMA treatment despite enhanced chromatin binding is also consistent with previous reports whereby it has been established that PMA-induced protein kinase (PK) C phosphorylation of PU.1 within its transactivation domain increases its binding capacity to a variety of PU.1 target genes [66, 67]. Hence, in the context of PrmIP, a model is presented in Fig 8C (i-ii) to illustrate the coordinated regulation of the PrmIP involving switching of nuclear factor binding of C/EBPδ to its *cis*-acting element, which mediates transcriptional repression under basal conditions, to binding of PU.1 to the PU.1(a) and PU.1(b) elements, to mediate transcriptional activation in response to PMA. It is proposed that as C/EBPδ expression and binding is decreased in response to PMA-induced differentiation, thereby lifting transcriptional repression and, consistent with previous data [66, 67], that the phosphorylation status and binding capacity of PU.1 is increased, favouring transcriptional activation.

In PRR2, mutational analysis established that the Sp1, PU.1 and Oct-1 sites, located at -965, -952 and -947 respectively, function independently to mediate the PMA-induced increase in hIP gene expression in this region. Sp1, a member of the family of Sp1-like/KLF factors, serves as a key component of the eukaryotic transcriptional apparatus [68]. It has been previously established that Sp1 binds to a GC-rich element within the core region of PrmIP and that PU.1 and Oct1 are further recruited to drive basal expression of the hIP gene [31] (see also Fig 8A). Oct-1 belongs to the Pit-Oct-Unc (POU) family of nuclear factors which bind to target sequences through their bipartite POU domains [69, 70] to regulate RNA

polymerase II (POLII)-dependent transcription of various genes in conjunction with specific co-activators [71, 72]. ChIP analysis corroborated previous reports that Sp1, PU.1 and Oct-1 bind to the core PrmIP under basal conditions [31] but also established that, in all cases, binding of these factors to the chromatin *in vivo* was substantially increased in a time-dependent manner in response to PMA. Moreover, similar to PU.1 and Oct-1, we have previously established that expression of Sp1 is unaffected by PMA treatment of HEL cells [37] but its DNA binding affinity and capacity is enhanced due to PMA-induced ERK phosphorylation of Sp1 [73-75] In the case of Oct-1, while it has been implicated in mediating the PMA induction of the human-interleukin (IL)-5 gene promoter in the mouse EL4 T cell line [76], the mechanism whereby phorbol esters increase Oct-1 binding to its target *cis*-acting DNA elements remains to be established. In the context of PrmIP, it is proposed that binding of Sp1, PU.1 and Oct-1 to the PRR2, which overlaps with the proximal core PrmIP region, is increased in response to PMA treatment of HEL cells, thereby further enhancing Sp1, PU.1 and Oct-1 regulation of the POLII-dependent transcription initiation apparatus (Fig 8C (iii)).

In conclusion, it has been established that C/EBPδ is a critical transcriptional regulator of PrmIP which, along with PU.1, binds to the URR within PrmIP to repress transcription of the hIP gene in HEL cells under basal conditions. Additionally, PMA-mediated differentiation of HEL cells upregulates hIP mRNA and PrmIP-directed gene expression. The PMA responsiveness of PrmIP has been localised to 2 specific regions, referred to as PRR1 and PRR2 which overlap/co-localize with the URR and core PrmIP regions, respectively. PMA induction of PrmIP is mediated by a combined switch from (a) predominantly C/EBPδ binding to the URR under the repressed state to predominantly PU.1 binding to the PMA-activated PRR1, in addition to (b) PMA-induced enhanced binding of the Sp1, PU.1 and Oct-1 multi-component positive regulatory complex to the PRR2/core PrmIP region. It is possible that these findings in HEL cells are universal amongst all megakaryocyte cell lines, and may indeed be the case in other model cell lines, although this has not yet been established. Taken together, these data provide further critical insights into transcriptional regulation of the hIP gene and thereby provide a strong genetic basis for understanding the many diverse physiological functions of prostacyclin and the hIP, including its involvement in CVD/CAD.

ACKNOWLEDGEMENTS:
This work was supported by Science Foundation Ireland and The Health Research Board, Ireland. pCMV5:C/EBPδ [34] was generously donated by Professor A-Mei Huang, Kaohsiung Medical University, Taiwan.

CONFLICT OF INTEREST: No aspect of this study has been subject to previous publication and no issues of conflict of interest occur.

REFERENCES:

[1] S. Narumiya, Y. Sugimoto, F. Ushikubi, Prostanoid receptors: structures, properties, and functions, Physiol Rev 79 (1999) 1193-1226.

[2] D.F. Woodward, R.L. Jones, S. Narumiya, International union of basic and clinical pharmacology. LXXXIII: classification of prostanoid receptors, updating 15 years of progress, Pharmacol Rev 63 (2011) 471-538.

[3] R.J. Gryglewski, Prostacyclin among prostanoids, Pharmacol Rep 60 (2008) 3-11.

[4] J. Kawabe, F. Ushikubi, N. Hasebe, Prostacyclin in vascular diseases. - Recent insights and future perspectives, Circ J 74 (2010) 836-843.

[5] K. Yuhki, H. Kashiwagi, F. Kojima, J. Kawabe, F. Ushikubi, Roles of prostanoids in the pathogenesis of cardiovascular diseases, Int Angiol 29 (2010) 19-27.

[6] R.J. Bing, Myocardial ischemia and infarction: growth of ideas, Cardiovasc Res 51 (2001) 13-20.

[7] N.N. Kahn, H.S. Mueller, A.K. Sinha, Impaired prostaglandin E1/I2 receptor activity of human blood platelets in acute ischemic heart disease, Circ Res 66 (1990) 932-940.

[8] A.M. Lefer, Prostacyclin, high density lipoproteins, and myocardial ischemia, Circulation 81 (1990) 2013-2015.

[9] T. Murata, F. Ushikubi, T. Matsuoka, M. Hirata, A. Yamasaki, Y. Sugimoto, A. Ichikawa, Y. Aze, T. Tanaka, N. Yoshida, A. Ueno, S. Oh-ishi, S. Narumiya, Altered pain perception and inflammatory response in mice lacking prostacyclin receptor, Nature 388 (1997) 678-682.

[10] Y. Sugimoto, S. Narumiya, A. Ichikawa, Distribution and function of prostanoid receptors: studies from knockout mice, Prog Lipid Res 39 (2000) 289-314.

[11] K.R. Bley, J.C. Hunter, R.M. Eglen, J.A. Smith, The role of IP prostanoid receptors in inflammatory pain, Trends Pharmacol Sci 19 (1998) 141-147.

[12] V.L. Roger, A.S. Go, D.M. Lloyd-Jones, R.J. Adams, J.D. Berry, T.M. Brown, M.R. Carnethon, S. Dai, G. de Simone, E.S. Ford, C.S. Fox, H.J. Fullerton, C. Gillespie, K.J. Greenlund, S.M. Hailpern, J.A. Heit, P.M. Ho, V.J. Howard, B.M. Kissela, S.J. Kittner, D.T. Lackland, J.H. Lichtman, L.D. Lisabeth, D.M. Makuc, G.M. Marcus, A. Marelli, D.B. Matchar, M.M. McDermott, J.B. Meigs, C.S. Moy, D. Mozaffarian, M.E. Mussolino, G. Nichol, N.P. Paynter, W.D. Rosamond, P.D. Sorlie, R.S. Stafford, T.N. Turan, M.B. Turner, N.D. Wong, J. Wylie-Rosett, Heart disease and stroke statistics--2011 update: a report from the American Heart Association, Circulation 123 (2011) e18-e209.

[13] T. Kobayashi, Y. Tahara, M. Matsumoto, M. Iguchi, H. Sano, T. Murayama, H. Arai, H. Oida, T. Yurugi-Kobayashi, J.K. Yamashita, H. Katagiri, M. Majima, M. Yokode, T. Kita, S. Narumiya, Roles of thromboxane A(2) and prostacyclin in the development of atherosclerosis in apoE-deficient mice, J Clin Invest 114 (2004) 784-794.

[14] J. Kawabe, K. Yuhki, M. Okada, T. Kanno, A. Yamauchi, N. Tashiro, T. Sasaki, S. Okumura, N. Nakagawa, Y. Aburakawa, N. Takehara, T. Fujino, N. Hasebe, S. Narumiya, F. Ushikubi, Prostaglandin I2 promotes recruitment of endothelial progenitor cells and limits vascular remodeling, Arterioscler Thromb Vasc Biol 30 (2010) 464-470.

[15] E.C. Turner, B.T. Kinsella, Estrogen increases expression of the human prostacyclin receptor within the vasculature through an ERalpha-dependent mechanism, J Mol Biol 396 (2010) 473-486 (Corrigendum, J Mol Biol (2011), 2413, 2899).

[16] O.A. Lawler, S.M. Miggin, B.T. Kinsella, Protein kinase A-mediated phosphorylation of serine 357 of the mouse prostacyclin receptor regulates its coupling to G(s)-, to G(i)-, and to G(q)-coupled effector signaling, J Biol Chem 276 (2001) 33596-33607.

[17] S.M. Miggin, B.T. Kinsella, Investigation of the mechanisms of G protein: effector coupling by the human and mouse prostacyclin receptors. Identification of critical species-dependent differences, J Biol Chem 277 (2002) 27053-27064.

[18] O.A. Lawler, S.M. Miggin, B.T. Kinsella, The effects of the statins lovastatin and cerivastatin on signalling by the prostanoid IP-receptor, Br J Pharmacol 132 (2001) 1639-1649.

[19] S.M. Miggin, O.A. Lawler, B.T. Kinsella, Investigation of a functional requirement for isoprenylation by the human prostacyclin receptor, Eur J Biochem 269 (2002) 1714-1725.

[20] S.M. Miggin, O.A. Lawler, B.T. Kinsella, Palmitoylation of the human prostacyclin receptor. Functional implications of palmitoylation and isoprenylation, J Biol Chem 278 (2003) 6947-6958.

[21] P.D. Donnellan, C.C. Kimbembe, H.M. Reid, B.T. Kinsella, Identification of a novel endoplasmic reticulum export motif within the eighth alpha-helical domain (alpha-H8) of the human prostacyclin receptor, Biochim Biophys Acta 1808 (2011) 1202-1218.

[22] P.D. Donnellan, B.T. Kinsella, Immature and mature species of the human Prostacyclin Receptor are ubiquitinated and targeted to the 26S proteasomal or lysosomal degradation pathways, respectively, J Mol Signal 4 (2009) 7.

[23] M.B. O'Keeffe, H.M. Reid, B.T. Kinsella, Agonist-dependent internalization and trafficking of the human prostacyclin receptor: a direct role for Rab5a GTPase, Biochim Biophys Acta 1783 (2008) 1914-1928.

[24] H.M. Reid, E.P. Mulvaney, E.C. Turner, B.T. Kinsella, Interaction of the human prostacyclin receptor with Rab11: characterization of a novel Rab11 binding domain within alpha-helix 8 that is regulated by palmitoylation, J Biol Chem 285 (2010) 18709-18726.

[25] K. Wikstrom, H.M. Reid, M. Hill, K.A. English, M.B. O'Keeffe, C.C. Kimbembe, B.T. Kinsella, Recycling of the human prostacyclin receptor is regulated through a direct interaction with Rab11a GTPase, Cell Signal 20 (2008) 2332-2346.

[26] E.C. Turner, E.P. Mulvaney, H.M. Reid, B.T. Kinsella, Interaction of the human prostacyclin receptor with the PDZ adapter protein PDZK1: role in endothelial cell migration and angiogenesis, Mol Biol Cell 22 (2011) 2664-2679.

[27] C. Midgett, J. Stitham, K.A. Martin, J. Hwa, Prostacyclin Receptor Regulation - From Transcription to Trafficking, Curr Mol Med 11 (2011) 517-528.

[28] P. Patrignani, C. Di Febbo, S. Tacconelli, K. Douville, M.D. Guglielmi, R.J. Horvath, M. Ding, K. Sierra, J. Stitham, S. Gleim, G. Baccante, V. Moretta, L. Di Francesco, M.L. Capone, E. Porreca, J. Hwa, Differential association between human prostacyclin receptor polymorphisms and the development of venous thrombosis and intimal hyperplasia: a clinical biomarker study, Pharmacogenet Genomics 18 (2008) 611-620.

[29] J. Stitham, E. Arehart, L. Elderon, S.R. Gleim, K. Douville, Z. Kasza, K. Fetalvero, T. MacKenzie, J. Robb, K.A. Martin, J. Hwa, Comprehensive biochemical analysis of rare prostacyclin receptor variants: study of association of signaling with coronary artery obstruction, J Biol Chem 286 (2011) 7060-7069.

[30] S. Saito, A. Iida, A. Sekine, S. Kawauchi, S. Higuchi, C. Ogawa, Y. Nakamura, Catalog of 178 variations in the Japanese population among eight human genes encoding G protein-coupled receptors (GPCRs), J Hum Genet 48 (2003) 461-468.

[31] E.C. Turner, B.T. Kinsella, Transcriptional regulation of the human prostacyclin receptor gene is dependent on Sp1, PU.1 and Oct-1 in megakaryocytes and endothelial cells, J Mol Biol 386 (2009) 579-597.

[32] M.W. Long, C.H. Heffner, J.L. Williams, C. Peters, E.V. Prochownik, Regulation of megakaryocyte phenotype in human erythroleukemia cells, J Clin Invest 85 (1990) 1072-1084.

[33] A.T. Coyle, B.T. Kinsella, Characterization of promoter 3 of the human thromboxane A receptor gene. A functional AP-1 and octamer motif are required for basal promoter activity, FEBS J 272 (2005) 1036-1053.

[34] M. Thangaraju, S. Ananth, P.M. Martin, P. Roon, S.B. Smith, E. Sterneck, P.D. Prasad, V. Ganapathy, c/ebpdelta Null mouse as a model for the double knock-out of slc5a8 and slc5a12 in kidney, J Biol Chem 281 (2006) 26769-26773.

[35] K.J. Livak, T.D. Schmittgen, Analysis of relative gene expression data using real-time quantitative PCR and the 2(-Delta Delta C(T)) Method, Methods 25 (2001) 402-408.

[36] A.M. Gannon, B.T. Kinsella, Regulation of the human thromboxane A2 receptor gene by Sp1, Egr1, NF-E2, GATA-1, and Ets-1 in megakaryocytes, J Lipid Res 49 (2008) 2590-2604.

[37] A.M. Gannon, E.C. Turner, H.M. Reid, B.T. Kinsella, Regulated expression of the alpha isoform of the human thromboxane A2 receptor during megakaryocyte differentiation: a coordinated role for WT1, Egr1, and Sp1, J Mol Biol 394 (2009) 29-45.

[38] J. Chen, M. Zhao, R. Rao, H. Inoue, C.M. Hao, C/EBP{beta} and its binding element are required for NF{kappa}B-induced COX2 expression following hypertonic stress, J Biol Chem 280 (2005) 16354-16359.

[39] Y.C. Pan, C.F. Li, C.Y. Ko, M.H. Pan, P.J. Chen, J.T. Tseng, W.C. Wu, W.C. Chang, A.M. Huang, E. Sterneck, J.M. Wang, CEBPD reverses RB/E2F1-mediated gene repression and participates in HMDB-induced apoptosis of cancer cells, Clin Cancer Res 16 (2010) 5770-5780.

[40] C.Y. Ko, H.C. Hsu, M.R. Shen, W.C. Chang, J.M. Wang, Epigenetic silencing of CCAAT/enhancer-binding protein delta activity by YY1/polycomb group/DNA methyltransferase complex, J Biol Chem 283 (2008) 30919-30932.

[41] K. Quandt, K. Frech, H. Karas, E. Wingender, T. Werner, MatInd and MatInspector: new fast and versatile tools for detection of consensus matches in nucleotide sequence data, Nucleic Acids Res 23 (1995) 4878-4884.

[42] D.P. Ramji, P. Foka, CCAAT/enhancer-binding proteins: structure, function and regulation, Biochem J 365 (2002) 561-575.

[43] J.J. Chen, W.C. Huang, C.C. Chen, Transcriptional regulation of cyclooxygenase-2 in response to proteasome inhibitors involves reactive oxygen species-mediated signaling pathway and recruitment of CCAAT/enhancer-binding protein delta and CREB-binding protein, Mol Biol Cell 16 (2005) 5579-5591.

[44] Y. Zhu, M.A. Saunders, H. Yeh, W.G. Deng, K.K. Wu, Dynamic regulation of cyclooxygenase-2 promoter activity by isoforms of CCAAT/enhancer-binding proteins, J Biol Chem 277 (2002) 6923-6928.

[45] Y. Kitami, T. Fukuoka, K. Hiwada, T. Inagami, A high level of CCAAT-enhancer binding protein-delta expression is a major determinant for markedly elevated differential gene expression of the platelet-derived growth factor-alpha receptor in vascular smooth muscle cells of genetically hypertensive rats, Circ Res 84 (1999) 64-73.

[46] S.R. Farmer, Regulation of PPARgamma activity during adipogenesis, Int J Obes (Lond) 29 Suppl 1 (2005) S13-16.

[47] A.M. Gannon, B.T. Kinsella, The Wilms' tumour suppressor protein WT1 acts as a key transcriptional repressor of the human thromboxane A2 receptor gene in megakaryocytes, J Cell Mol Med 13 (2009) 4571-4586.

[48] S. Ibrahim, M. Tetruashvily, A.J. Frey, S.J. Wilson, J. Stitham, J. Hwa, E.M. Smyth, Dominant negative actions of human prostacyclin receptor variant through dimerization: implications for cardiovascular disease, Arterioscler Thromb Vasc Biol 30 (2010) 1802-1809.

[49] S. Carotta, L. Wu, S.L. Nutt, Surprising new roles for PU.1 in the adaptive immune response, Immunol Rev 238 (2010) 63-75.
[50] S.R. McKercher, B.E. Torbett, K.L. Anderson, G.W. Henkel, D.J. Vestal, H. Baribault, M. Klemsz, A.J. Feeney, G.E. Wu, C.J. Paige, R.A. Maki, Targeted disruption of the PU.1 gene results in multiple hematopoietic abnormalities, EMBO J 15 (1996) 5647-5658.
[51] P. Burda, P. Laslo, T. Stopka, The role of PU.1 and GATA-1 transcription factors during normal and leukemogenic hematopoiesis, Leukemia 24 (2010) 1249-1257.
[52] A.D. Friedman, Transcriptional regulation of granulocyte and monocyte development, Oncogene 21 (2002) 3377-3390.
[53] A.D. Friedman, Transcriptional control of granulocyte and monocyte development, Oncogene 26 (2007) 6816-6828.
[54] S. Nagulapalli, J.M. Pongubala, M.L. Atchison, Multiple proteins physically interact with PU.1. Transcriptional synergy with NF-IL6 beta (C/EBP delta, CRP3), J Immunol 155 (1995) 4330-4338.
[55] M. Joo, M. Kwon, Y.J. Cho, N. Hu, T.V. Pedchenko, R.T. Sadikot, T.S. Blackwell, J.W. Christman, Lipopolysaccharide-dependent interaction between PU.1 and c-Jun determines production of lipocalin-type prostaglandin D synthase and prostaglandin D2 in macrophages, Am J Physiol Lung Cell Mol Physiol 296 (2009) L771-779.
[56] A.A. Yee, P. Yin, D.P. Siderovski, T.W. Mak, D.W. Litchfield, C.H. Arrowsmith, Cooperative interaction between the DNA-binding domains of PU.1 and IRF4, J Mol Biol 279 (1998) 1075-1083.
[57] M.A. Smith, G. Wright, J. Wu, P. Tailor, K. Ozato, X. Chen, S. Wei, J.F. Piskurich, J.P. Ting, K.L. Wright, Positive regulatory domain I (PRDM1) and IRF8/PU.1 counter-regulate MHC class II transactivator (CIITA) expression during dendritic cell maturation, J Biol Chem 286 (2011) 7893-7904.
[58] W. Huang, E. Horvath, E.A. Eklund, PU.1, interferon regulatory factor (IRF) 2, and the interferon consensus sequence-binding protein (ICSBP/IRF8) cooperate to activate NF1 transcription in differentiating myeloid cells, J Biol Chem 282 (2007) 6629-6643.
[59] F. Kihara-Negishi, M. Suzuki, T. Yamada, T. Sakurai, T. Oikawa, Impaired repressor activity and biological functions of PU.1 in MEL cells induced by mutations in the acetylation motifs within the ETS domain, Biochem Biophys Res Commun 335 (2005) 477-484.
[60] T.N. Cassel, M. Nord, C/EBP transcription factors in the lung epithelium, Am J Physiol Lung Cell Mol Physiol 285 (2003) L773-781.
[61] M. Centrella, S. Christakos, T.L. McCarthy, Skeletal hormones and the C/EBP and Runx transcription factors: interactions that integrate and redefine gene expression, Gene 342 (2004) 13-24.
[62] G.J. Darlington, S.E. Ross, O.A. MacDougald, The role of C/EBP genes in adipocyte differentiation, J Biol Chem 273 (1998) 30057-30060.
[63] M. Takiguchi, The C/EBP family of transcription factors in the liver and other organs, Int J Exp Pathol 79 (1998) 369-391.
[64] S. Kinoshita, S. Akira, T. Kishimoto, A member of the C/EBP family, NF-IL6 beta, forms a heterodimer and transcriptionally synergizes with NF-IL6, Proc Natl Acad Sci U S A 89 (1992) 1473-1476.
[65] H.W. Shen, Y.L. Chen, C.Y. Chern, W.M. Kan, The effect of prostacyclin agonists on the differentiation of phorbol ester treated human erythroleukemia cells, Prostaglandins Other Lipid Mediat 83 (2007) 231-236.
[66] J.O. Carey, K.J. Posekany, J.E. deVente, G.R. Pettit, D.K. Ways, Phorbol ester-stimulated phosphorylation of PU.1: association with leukemic cell growth inhibition, Blood 87 (1996) 4316-4324.
[67] M. Hamdorf, A. Berger, S. Schule, J. Reinhardt, E. Flory, PKCdelta-Induced PU.1 Phosphorylation Promotes Hematopoietic Stem Cell Differentiation to Dendritic Cells, Stem Cells 29 (2011) 297-306.
[68] L. Li, S. He, J.M. Sun, J.R. Davie, Gene regulation by Sp1 and Sp3, Biochem Cell Biol 82 (2004) 460-471.
[69] R.A. Sturm, G. Das, W. Herr, The ubiquitous octamer-binding protein Oct-1 contains a POU domain with a homeo box subdomain, Genes Dev 2 (1988) 1582-1599.
[70] M.M. Muller, S. Ruppert, W. Schaffner, P. Matthias, A cloned octamer transcription factor stimulates transcription from lymphoid-specific promoters in non-B cells, Nature 336 (1988) 544-551.
[71] M. Strubin, J.W. Newell, P. Matthias, OBF-1, a novel B cell-specific coactivator that stimulates immunoglobulin promoter activity through association with octamer-binding proteins, Cell 80 (1995) 497-506.
[72] M. Tanaka, J.S. Lai, W. Herr, Promoter-selective activation domains in Oct-1 and Oct-2 direct differential activation of an snRNA and mRNA promoter, Cell 68 (1992) 755-767.
[73] A.P. Kumar, A.P. Butler, Serum responsive gene expression mediated by Sp1, Biochem Biophys Res Commun 252 (1998) 517-523.
[74] M. Liao, Y. Zhang, M.L. Dufau, Protein kinase Calpha-induced derepression of the human luteinizing hormone receptor gene transcription through ERK-mediated release of HDAC1/Sin3A repressor complex from Sp1 sites, Mol Endocrinol 22 (2008) 1449-1463.
[75] J.H. Tsou, K.Y. Chang, W.C. Wang, J.T. Tseng, W.C. Su, L.Y. Hung, W.C. Chang, B.K. Chen, Nucleolin regulates c-Jun/Sp1-dependent transcriptional activation of cPLA2alpha in phorbol ester-treated non-small cell lung cancer A549 cells, Nucleic Acids Res 36 (2008) 217-227.
[76] V. Gruart-Gouilleux, P. Engels, M. Sullivan, Characterization of the human interleukin-5 gene promoter: involvement of octamer binding sites in the gene promoter activity, Eur J Immunol 25 (1995) 1431-1435.

FIGURES

Figure 1. Identification of an upstream repressor region (URR) and putative PU.1 and C/EBP *cis*-acting elements within PrmIP

Panel A: A schematic of the human prostacyclin receptor (IP) genomic region spanning nucleotides -2449 to +767 encoding PrmIP, where the relative positions of exon (E) 1, intron (I) 1 and E2, is shown. Nucleotide +1 corresponds to the translational start site (ATG) and the transcription initiation (TI) site is at -916. Recombinant pGL3B plasmids encoding PrmIP (-2449 to -772), PrmIP4 (-1524 to -772) and PrmIP5 (-1293 to -772) or, as controls, pGL3Control and pGL3B were co-transfected with pRL-TK into HEL 92.1.7 cells. Panel B: A schematic of PrmIP4 showing the positions of putative p53, PU.1 (-1454, designated PU.1 (a)), STAT, PU.1 (-1375, designated PU.1 (b)), NFκB (-1356, designated NFκB (a)), NFκB (-1359, designated NFκB (b)), Nrf1, C/EBP and C-LH elements. Panel C: A schematic of PrmIP4 showing the positions of putative PU.1(a), PU.1(b) and C/EBP elements. In panels (B) and (C), the 5' nucleotide of each *cis*-acting element is indicated and the star symbol indicates mutated elements. pGL3B plasmids encoding PrmIP4, PrmIP5 or the indicated mutated derivatives of PrmIP4 were co-transfected with pRL-TK into HEL cells. Cells in panels A-C were assayed for luciferase activity 48 hr post-transfection and results are expressed as mean firefly relative to renilla luciferase activity, expressed in arbitrary RLU (± SEM, $n \geq 6$). The asterisks indicate that deletion (A) or mutation (B & C) of PrmIP sequences significantly increased reporter gene expression in HEL cells, where **, *** and **** indicate $p \leq 0.01$, 0.001 and 0.0001, respectively.

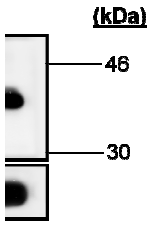

Fig 2. *In vivo* binding and expression of C/EBPβ, C/EBPδ and PU.1 in HEL cells.
Panels A & B: Chromatin immunoprecipitation (ChIP) analysis of C/EBPβ, C/EBPδ and PU.1 binding to PrmIP, using either input chromatin or chromatin extracted from *anti*-C/EBPβ, *anti*-C/EBPδ, *anti*-PU.1 or normal rabbit IgG immunoprecipitates or, as an additional control, from immunoprecipitates generated in the absence of primary (1°) antibody (- AB). PCR analysis was performed using (A) primers to amplify the -1528 to -1327 region (indicated by solid arrows) or, (B) as a negative control, primers to amplify the -1761 to -1577 region of PrmIP (indicated by dashed arrows). Panel C: Real time quantitative (QT) - PCR quantitation of the (i) URR and (ii) negative control ChIP data where the bar charts shows mean levels of PCR product generated from the individual test or control immunoprecipitates expressed as a percentage relative to those levels derived from the corresponding input chromatins. Panel D: Immunoblot analysis of (i) C/EBPβ, (ii) C/EBPδ, and (iii) PU.1 expression in HEL cells (50μg whole cell protein analysed per lane), where blots were re-screened using an *anti*-HDJ2 antibody to confirm uniform protein loading. The molecular size markers (kDa) are indicated to the right of the panels. Images in panels A – D are representative of three independent experiments.

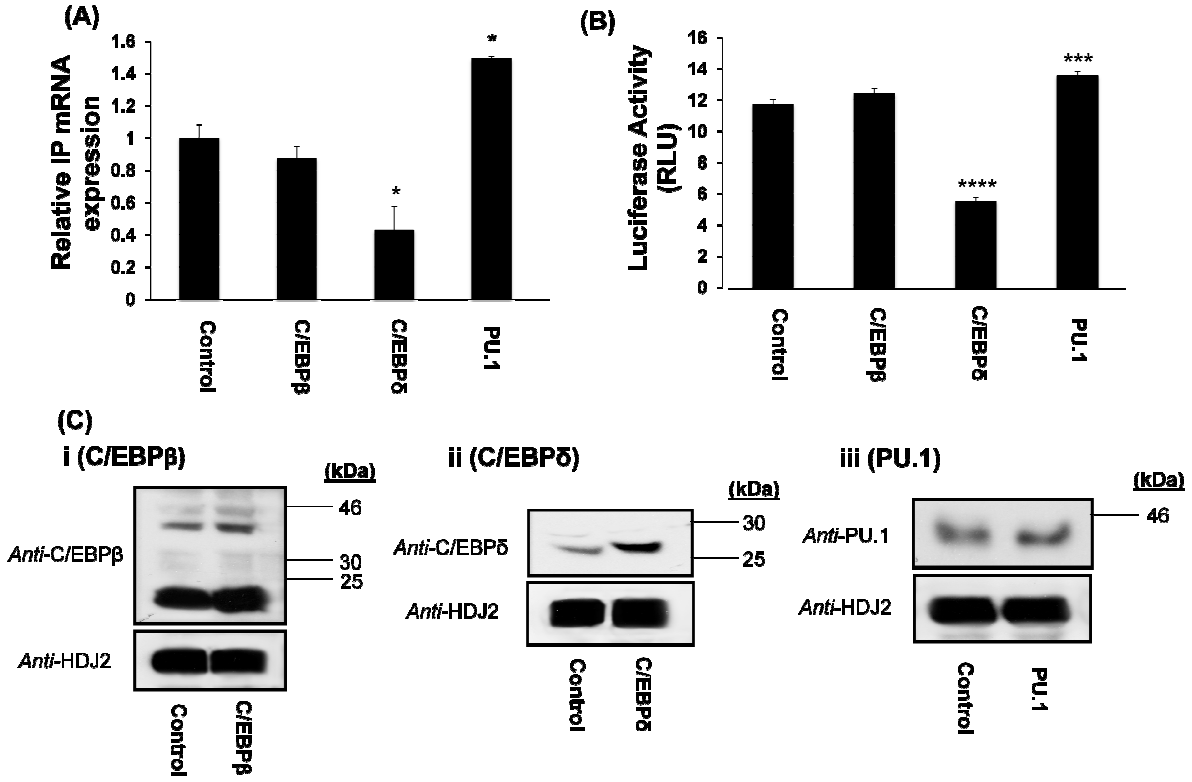

Fig 3. Effect of C/EBPβ, C/EBPδ and PU.1 on hIP mRNA and PrmIP-directed gene expression.
Panel A: HEL cells were transiently transfected with recombinant pCMV5 encoding C/EBPβ, C/EBPδ, PU.1 or, as a negative control, with vector alone (Control). Cells were harvested at 48 hr post-transfection and assayed by QT-PCR analysis to monitor hIP mRNA expression, normalised relative to 18s rRNA expression, levels. Data is presented as mean relative hIP mRNA expression levels (± SEM, n = 3), relative to those levels in pCMV5 control-transfected cells set to a value of 1. Panel B: HEL cells were transiently co-transfected with pGL3B:PrmIP4 plus pRL-TK in the presence of recombinant pCMV5 encoding C/EBPβ, C/EBPδ, PU.1 or, as a negative control, with vector alone (Control). Cells were assayed 48 hr post-transfection for mean luciferase activity (RLU ± SEM, $n \geq 6$). The asterisks indicate that ectopic expression of C/EBPδ decreased and of PU.1 increased hIP mRNA and luciferase reporter gene expression, where *, *** and **** indicate $p < 0.05$, 0.001 and 0.0001, respectively. Panel C: Immunoblot analysis (50 µg whole cell protein per lane) confirmed overexpression of (i) C/EBPβ, (ii) C/EBPδ and (iii) PU.1 protein in transfected HEL cells where blots were re-screened with *anti*-HDJ2 antisera to confirm uniform protein loading. The positions of the molecular size markers (kDa) are indicated to the right of the panels, and images are representative of three independent experiments.

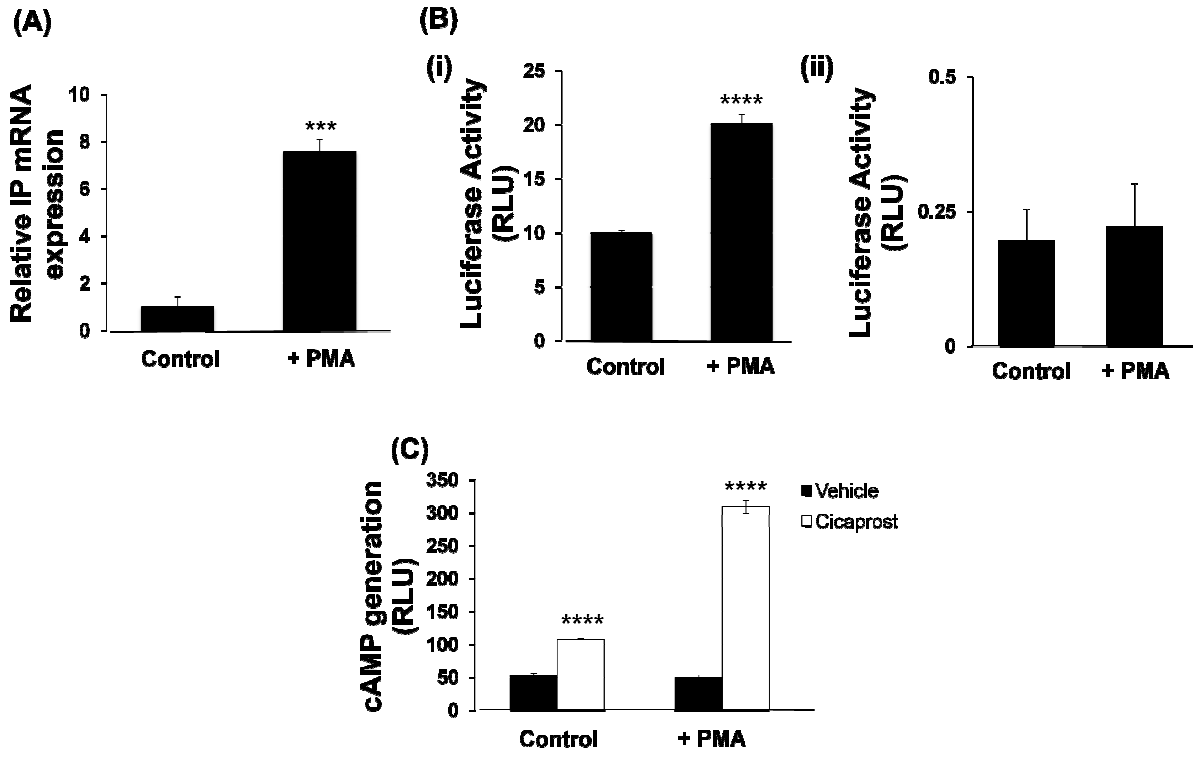

Fig 4. Effect of PMA on hIP mRNA levels, gene expression and cAMP generation in HEL cells.
Panel A: Real time QT-PCR analysis of hIP mRNA expression, normalised relative to 18s rRNA, in HEL cells incubated for 24 hr with either vehicle (0.1% DMSO; Control) or PMA (100 nM). Data is presented as mean fold increase in hIP mRNA expression in response to PMA relative to levels in vehicle-treated cells set to a value of 1 (± SEM, n = 3). Panel B: HEL cells were transiently co-transfected with pRL-TK in the presence of (i) pGL3B:PrmIP or, (ii) as a control, pGL3B. At 24 hr post transfection, cells were incubated for an additional 24 hr with either vehicle or PMA, prior to assaying for luciferase activity (RLU ± SEM, $n \geq 5$). Panel C: HEL cells were co-transfected with the pCRE-Luc (PMA-responsive) and pRL-TK (non-responsive) luciferase reporter plasmids, respectively. At 24 hr post-transfection, cells were incubated for an additional 24 hr with either vehicle or PMA. Levels of cAMP accumulation in response to stimulation of cells for 3 hr with either cicaprost (1 μM) or vehicle (PBS; Veh) were determined and expressed in arbitrary RLU (± SEM, n = 3). The asterisks in panels A - C indicate that PMA significantly increased hIP mRNA levels, luciferase reporter gene expression or cAMP generation, where *** and **** indicate $p < 0.001$ and 0.0001, respectively.

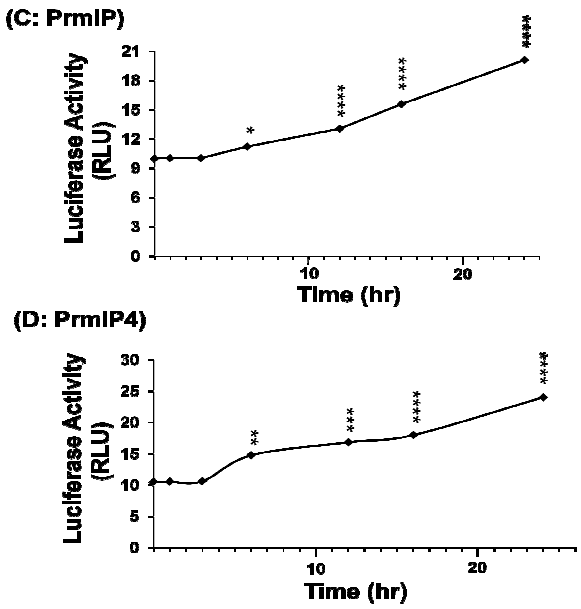
(C: PrmIP)
Luciferase Activity (RLU)
Time (hr)
(D: PrmIP4)
Luciferase Activity (RLU)
Time (hr)

Fig 5. Identification of two PMA-responsive regions (PRRs) within PrmIP.
Panels A & B: Recombinant pGL3B plasmids encoding PrmIP (-2449 to -772), and its 5' deletion derivatives PrmIP1-PrmIP7 or, as a control, pGL3B were co-transfected with pRL-TK into HEL cells. At 24 hr post-transfection, cells were incubated for an additional 24 hr with either the vehicle (0.1% DMSO) or PMA (100 nM), prior to assaying for luciferase activity (RLU ± SEM, $n \geq 5$). In panel A, data is presented as relative luciferase activity (RLU) and in panel B as the relative fold increase in PMA-induced luciferase activity. In A, the asterisks indicate where PMA induced significant increases in luciferase activity relative to levels in vehicle-treated cells while in B, they indicate where there are significant differences in the fold increases between adjacent fragments, where *** and **** indicate $p \leq 0.001$ and 0.0001, respectively. As indicated in panel B, two PMA-responsive regions (PRR) 1 and 2 were identified within the PrmIP. Panels C and D: HEL cells, transiently co-transfected with pRL-TK plus (C) pGL3B:PrmIP or (D) pGL3B:PrmIP4 were incubated with PMA (100nM) for 0 - 24 hr prior to harvesting 48 hr post-transfection. Cells were assayed for luciferase activity and results are expressed as mean luciferase activity (RLU ± SEM, $n \geq 4$). Data was analysed using two-way ANOVA and post hoc Dunnett's multiple comparison *t* test, which established that PMA treatment led to significant increases in both PrmIP- and PrmIP4-directed luciferase reporter gene expression, where *, **, *** and **** indicate $p \leq 0.05$, 0.01, 0.001 and 0.0001, respectively.

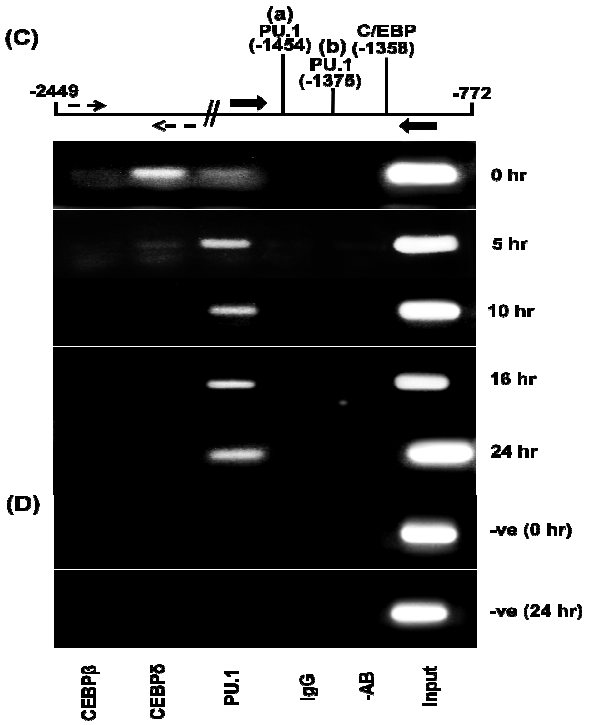
(C)
(a)
PU.1
(-1454)
(b)
PU.1
(-1375)
C/EBP
(-1358)
-2449
-772
0 hr
5 hr
10 hr
16 hr
24 hr
(D)
-ve (0 hr)
-ve (24 hr)
CEBPβ
CEBPδ
PU.1
IgG
-AB
Input

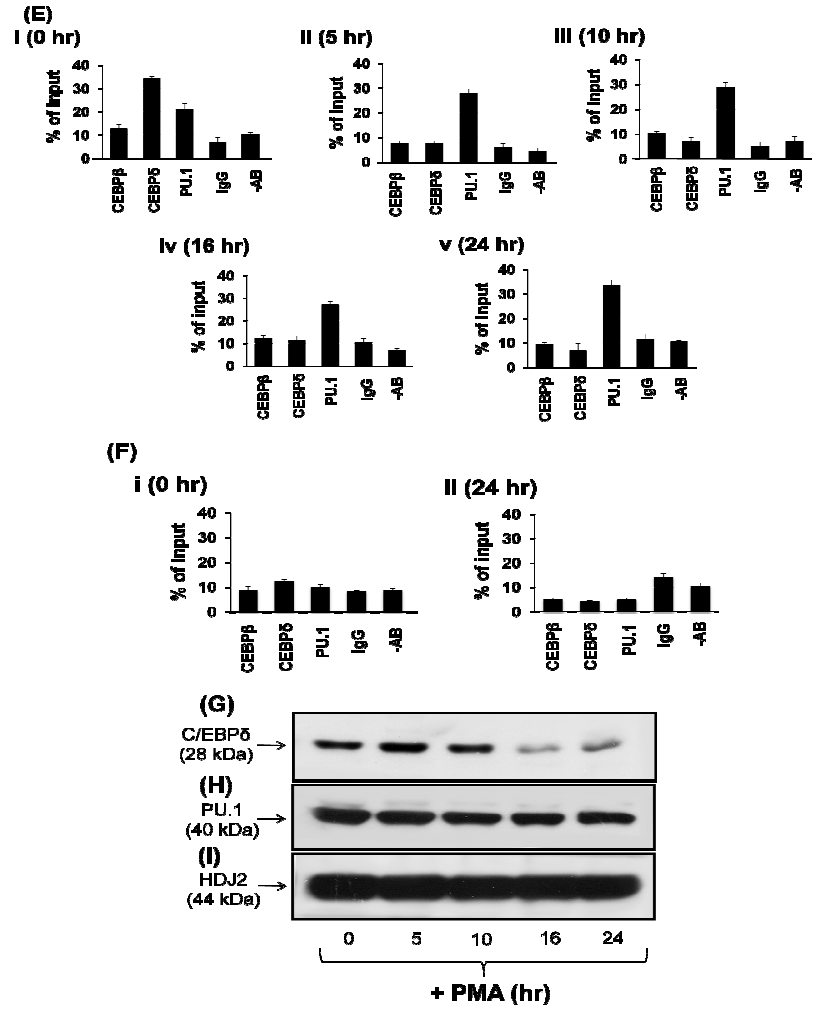

Fig 6. Characterisation of PRR1 within the PrmIP.
Panels A & B: A schematic of PrmIP4 showing the positions of the PU.1(a), PU.1(b) and C/EBP elements. Recombinant pGL3B plasmids encoding PrmIP4, PrmIP5 or the various mutated derivatives of PrmIP4 were co-transfected with pRL-TK into HEL cells. At 24 hr post-transfection, cells were incubated for an additional 24 hr with either vehicle (0.1% DMSO) or PMA (100 nM), prior to assaying for luciferase activity (RLU ± SEM, $n \geq 4$). In panel A, data is presented as relative luciferase activity (RLU) and in panel B as the relative fold increase in PMA-induced luciferase activity. In A, the asterisks indicate where PMA induced significant increases in luciferase activity relative to levels in vehicle-treated cells while in B, they indicate where there are significant differences in the fold increases between adjacent fragments, where *, *** and **** indicate $p \leq 0.05$, 0.001 and 0.0001, respectively. As indicated in panel B, disruption of the PU.1(a) or PU.1(b), but not the C/EBP element, reduced the PMA-response of PrmIP4 to that of PrmIP5. Panels C & D: ChIP analysis of C/EBPβ, C/EBPδ and PU.1 binding to PrmIP, using either input chromatin or chromatin extracted from *anti*-C/EBPβ, *anti*-C/EBPδ, *anti*-PU.1, normal rabbit IgG or no 1° antibody control immunoprecipitates from non-treated (0 hr) or PMA-treated (100 nM, 5, 10, 16 and 24 hr) HEL cells. PCR analysis was performed using primers to amplify the (C) -1528 to -1327 region (indicated by solid arrows) or, (D) as a negative control, primers to amplify the -1761 to -1577 region of PrmIP (indicated by dashed arrows). Panels E & F: Real time QT-PCR of the ChIP data presented in panels C & D, respectively, where the bar charts shows mean levels of PCR product generated from the individual test or control immunoprecipitates expressed as a percentage relative to those levels derived from the corresponding input chromatins from non-treated (0 hr) or PMA-treated (100 nM, 5, 10, 16 or 24 hr) HEL cells. Panels G-I: Immunoblot analysis of (G) C/EBPδ, (H) PU.1 and (I), as a loading control, HDJ2 expression following pre-incubation of HEL cells under non-treated (0 hr) or PMA-treated (100 nM; 5, 10, 16 and 24 hr) conditions. The molecular sizes (kDa) are indicated to the left of the panels. Images in panels C-I are representative of three independent experiments.

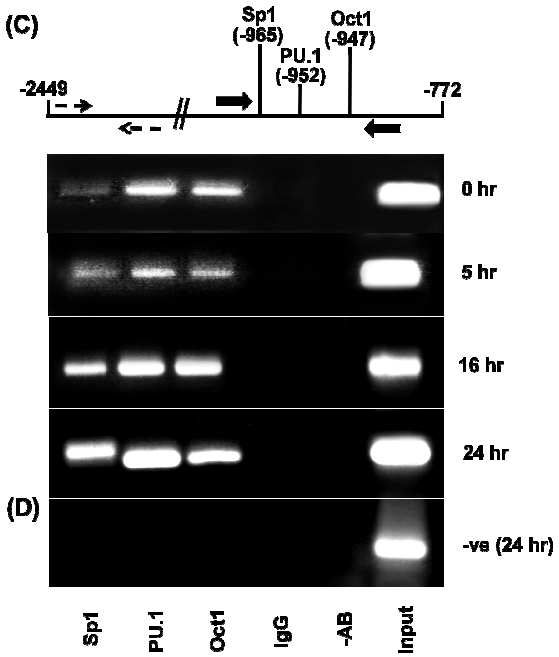
(C)
Sp1
(-965)
Oct1
(-947)
PU.1
(-952)
-2449
-772
0 hr
5 hr
16 hr
24 hr
(D)
-ve (24 hr)
Sp1
PU.1
Oct1
IgG
-AB
Input

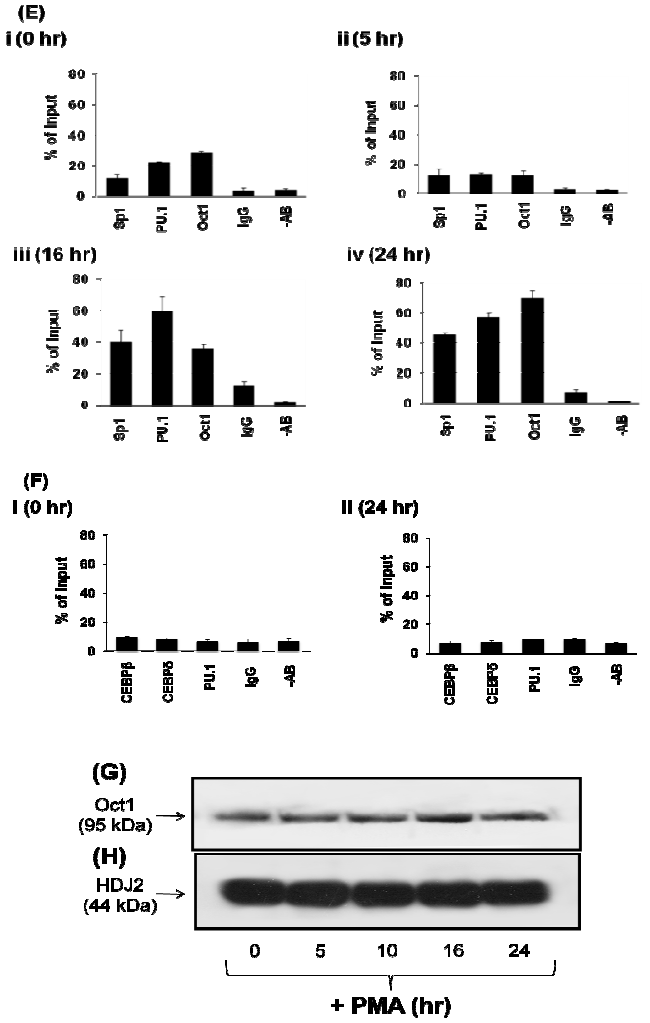

Fig 7. Characterisation of PRR2 within the PrmIP.
Panels A & B: A schematic of PrmIP6 showing the positions of the Sp1, PU.1 and Oct-1 elements. Recombinant pGL3B plasmids encoding PrmIP6, PrmIP7 or the various mutated derivatives of PrmIP6 were co-transfected with pRL-TK into HEL cells. At 24 hr post-transfection, cells were incubated for an additional 24 hr with either vehicle (0.1% DMSO) or PMA (100 nM), prior to assaying for luciferase activity (RLU ± SEM, $n \geq 5$). In panel A, data is presented as relative luciferase activity (RLU) and in panel B as the relative fold increase in PMA-induced luciferase activity. In A, the asterisks indicate where PMA induced significant increases in luciferase activity relative to levels in vehicle-treated cells while in B, they indicate where there are significant differences in the fold increases between adjacent fragments, where *, **, *** and **** indicate $p \leq 0.05$, 0.01, 0.001 and 0.0001, respectively. As indicated in panel B, combined disruption of the Sp1, PU.1 and Oct1 elements reduced the PMA response of PrmIP6 to that of PrmIP7. Panels C & D: ChIP analysis of Sp1, PU.1 and Oct-1 binding to PrmIP using either input chromatin or chromatin extracted from *anti*-Sp1, *anti*-PU.1, *anti*-Oct1, normal rabbit IgG or no 1° antibody control immunoprecipiates from non-treated (0 hr) or PMA-treated (100 nM, 5, 16 and 24 hr) HEL cells. PCR analysis was performed using primers to amplify the (C) -1263 to -827 region (indicated by solid arrows) or, (D) as a negative control, primers to amplify the -1761 to -1577 region of PrmIP (indicated by dashed arrows). Panels E & F: Real time QT-PCR of the ChIP data presented in panels C & D, respectively, where the bar charts shows mean levels of PCR product generated from the individual test or control immunoprecipitates expressed as a percentage relative to those levels derived from the corresponding input chromatins from non-treated (0 hr) or PMA-treated (100 nM, 5, 16 or 24 hr) HEL cells. Panels G & H: Immunoblot analysis of (G) Oct-1 and (H), as a loading control, HDJ2 expression following pre-incubation of HEL cells under non-treated (0 hr) or PMA-treated (100 nM, 5, 10, 16 and 24 hr) conditions. The molecular sizes (kDa) are indicated to the left of the panels. Images in panels C-H are representative of three independent experiments.

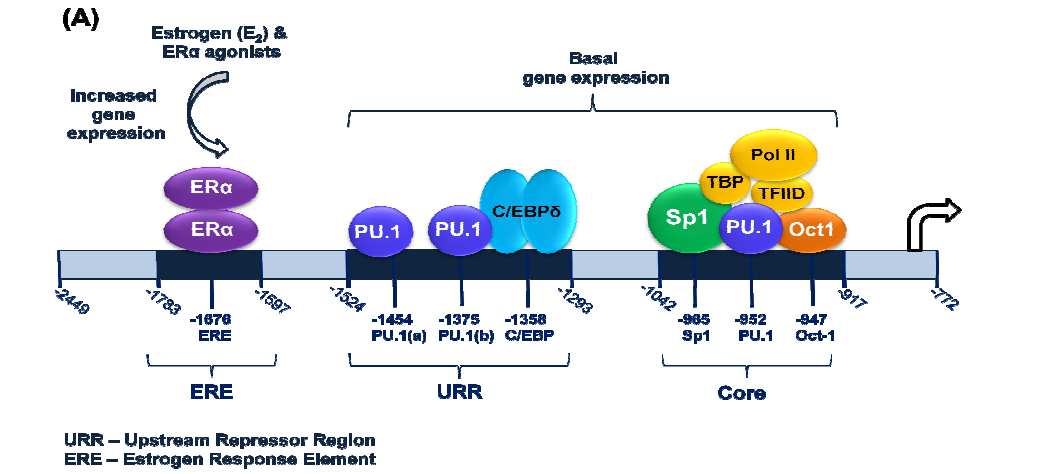
(A)
Estrogen (E2) & ERα agonists
Increased gene expression
Basal gene expression
ERα
ERα
PU.1
PU.1
C/EBPδ
Pol II
TBP
TFIID
Sp1
PU.1
Oct1
-2449
-1783
-1676 ERE
-1597
-1524
-1454 PU.1(a)
-1375 PU.1(b)
-1358 C/EBP
-1293
-1042
-965 Sp1
-952 PU.1
-947 Oct-1
-917
-772
ERE
URR
Core
URR – Upstream Repressor Region
ERE – Estrogen Response Element

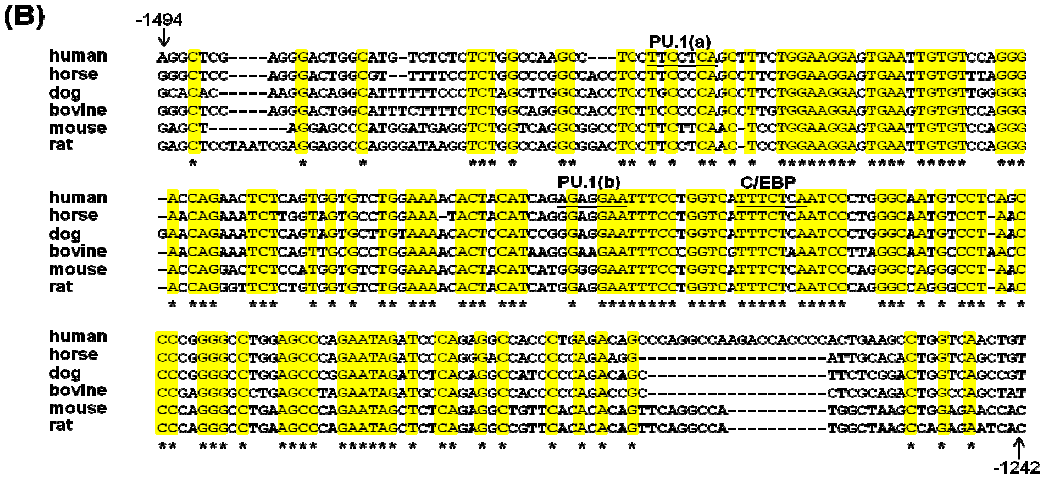
(B)
-1494
PU.1(a)
PU.1(b)
C/EBP
human
horse
dog
bovine
mouse
rat
-1242

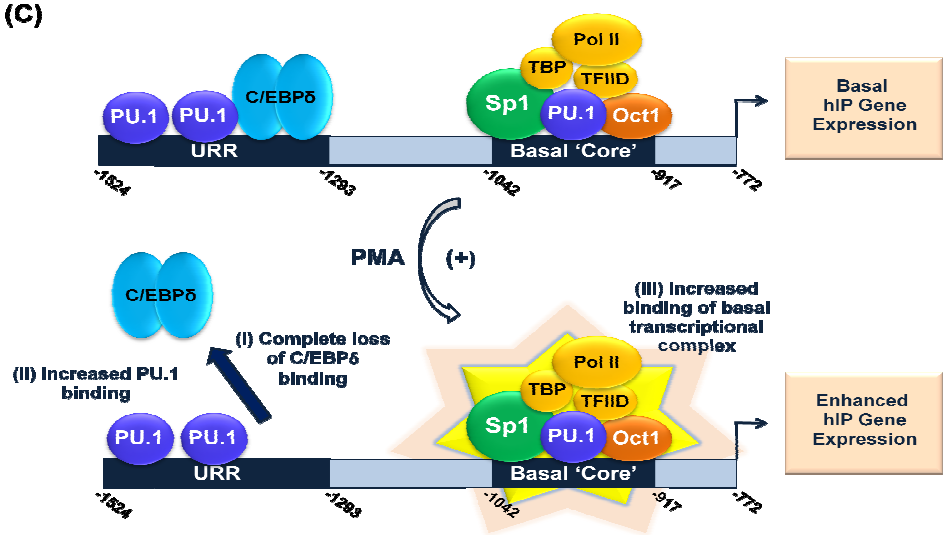
(C)
PU.1
PU.1
C/EBPδ
URR
Pol II
TBP
TFIID
Sp1
PU.1
Oct1
Basal 'Core'
-1524
-1293
-1042
-917
-772
Basal hIP Gene Expression
PMA
(+)
(I) Complete loss of C/EBPδ binding
(II) Increased PU.1 binding
(III) Increased binding of basal transcriptional complex
Enhanced hIP Gene Expression

Fig 8. Proposed models for PU.1-C/EBPδ cooperative binding and for PMA-mediated increases in PrmIP-directed gene expression.

Panel A: Schematic of PrmIP composed of three major regulatory regions including the previously identified estrogen-reponsive element (ERE) where ERα binds [15], and a core regulatory region, where Sp1, PU.1 and Oct-1 bind to regulate basal transcription of the hIP gene [31]. Herein, an upstream repressor region (URR), located between -1524 and -1293, was revealed within PrmIP where C/EBPδ and PU.1 bind to mediate transcriptional repression of hIP gene expression. More specifically, it is proposed that coordinated binding of a dimeric C/EBPδ molecule to the *cis*-acting C/EBP element at -1358 and of PU.1 to the adjacent PU.1(b) element at -1375 mediates transcriptional repression of PrmIP. Panel B: Sequence alignment of the URR of the human PrmIP (-1524 to -1293) with the equivalent regions from the horse, dog, bovine, mouse and rat IP promoter sequences. Fully conserved bases are indicated by asterisks and highlighted. The PU.1(a), PU.1(b) and C/EBP elements were found to be highly conserved throughout the species and are underlined. Panel C: Hypothetical scheme for PMA-induced changes in transcriptional regulator binding in PrmIP. As stated, under basal conditions, binding of C/EBPδ and PU.1 in the URR mediates repression of PrmIP expression. Following PMA-treatment of HEL cells, (i) there is a complete loss of C/EBPδ binding, alleviating transcriptional repression in this region. (ii) This loss of repression coincides with increased binding of PU.1 in URR, leading to enhanced transcriptional activation of PrmIP. (iii) Coincident with this, increased binding of Sp1, PU.1 and Oct-1 within the core/basal promoter region further enhances the PMA-induced transcriptional activation of PrmIP.

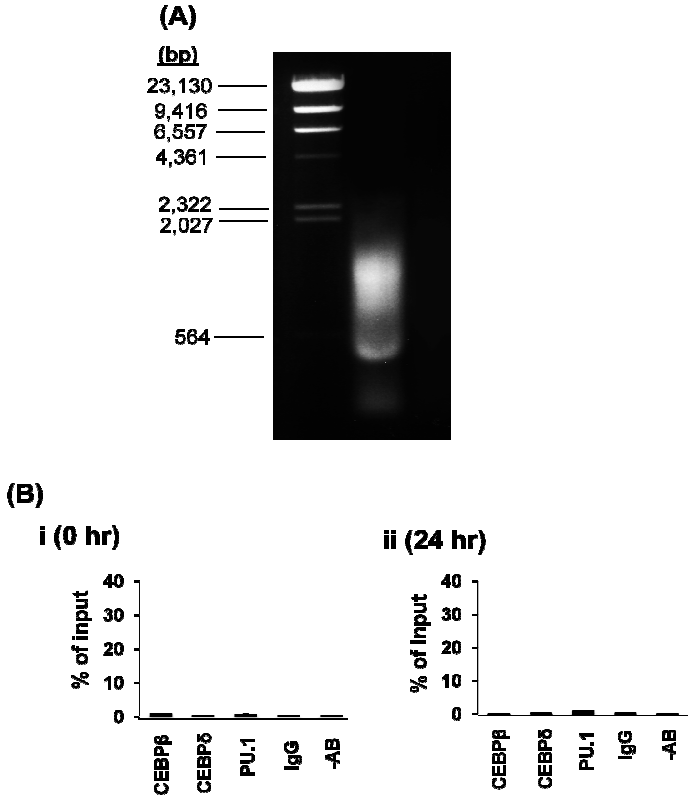

Supplemental Fig 1. Analysis of Sheared Input Chromatin-derived DNA and negative control QT-PCR in TP.

Panel A (i & ii): Agarose gel electrophoresis of two representative examples of sheared input chromatin-derived chromosomal DNA (~ 2.5 μg/lane). The fragments generated from Hind III digestion of bacteriophage lamhda (λ) DNA are also presented, where the relative sizes of fragments (bp) are indicated on the left of the gel image. It is estimated that the fragment sizes of the sheared chromatin DNA range from 350 – 1000 bp, with an average size of ~500 bp. Panel B (i & ii): Negative control real time QT-PCR analysis using primers specific to a region of Prm3 of the TP gene. The bar charts show mean levels of PCR product generated from the individual test or control immunoprecipitates expressed as a percentage relative to those levels derived from the corresponding input chromatins from non-treated (0 hr) or PMA-treated (100 nM, 24 hr) HEL cells.

Supplemental Fig 2. Further characterisation of PRR1 within PrmIP.
Panels A & B: A schematic of PrmIP4 showing the positions of the p53, STAT, NFκB(a), NFκB(b), Nrf1 and C-LH elements. Recombinant pGL3B plasmids encoding PrmIP4, PrmIP5 or the various mutated derivatives of PrmIP4 were co-transfected with pRL-TK into HEL cells. At 24 hr post-transfection, cells were incubated for an additional 24 hr with either vehicle (0.1% DMSO) or PMA (100 nM), prior to assaying for luciferase activity (RLU ± SEM, $n \geq 4$). In panel A, data is presented as relative luciferase activity (RLU) and in panel B as the relative fold increase in PMA-induced luciferase activity. In A, the asterisks indicate where PMA induced significant increases in luciferase activity relative to levels in vehicle-treated cells, where *** and **** indicate $p \leq 0.001$ and 0.0001, respectively. As indicated in panel B, disruption of the indicated elements had no significant effect on the PMA response of PrmIP4.